

SECOND-GENERATION OBJECTS IN THE UNIVERSE: RADIATIVE COOLING AND COLLAPSE OF HALOS WITH VIRIAL TEMPERATURES ABOVE 10^4 KELVIN

S. PENG OH

Theoretical Astrophysics, Mail Code 130-33, Caltech, Pasadena, CA, 91125, USA
peng@tapir.caltech.eduZOLTÁN HAIMAN¹Princeton University Observatory, Princeton, NJ 08544, USA
zoltan@astro.princeton.edu*Draft version October 29, 2018*

ABSTRACT

The first generation of stars is thought to have formed in low-mass halos with $T_{\text{vir}} < 10^4$ K where H₂ cooling is paramount. However, the efficiency of H₂ formation and cooling in these halos may have been severely limited by feedback processes. In this paper we investigate the radiative cooling and collapse of halos with virial temperatures $T_{\text{vir}} > 10^4$ K, i.e. those that can cool in the absence of H₂ via neutral atomic lines. The evolution of these halos differs from their less massive counterparts. Efficient atomic line radiation allows rapid cooling to ~ 8000 K; subsequently the gas can contract nearly isothermally at this temperature. In the absence of H₂ molecules, the gas would likely settle into a locally stable disk and only disks with unusually low spin would be unstable. However, we find that the initial atomic line cooling leaves a large, out-of-equilibrium residual free electron fraction. This allows the molecular fraction to build up to a universal value of $x_{\text{H}_2} \approx 10^{-3}$, almost independently of initial density and temperature. We show that this is a non-equilibrium freeze-out value that can be understood in terms of timescale arguments. Unlike in less massive halos, H₂ formation and cooling is largely impervious to feedback from external UV fields, due to the high initial densities achieved by atomic cooling. The newly formed molecules cool the gas further to ~ 100 K, and allow the gas to fragment on scales of a few $\times 100$ M_⊙. We investigate the importance of various feedback effects such as H₂ photodissociation from internal UV fields and radiation pressure due to Ly α photon trapping, which are likely to regulate the efficiency of star formation.

Subject headings: cosmology: theory – early universe – galaxies: formation – molecular processes

1. INTRODUCTION

The first generation of stars and/or quasars must have formed out of gas with primordial composition dictated by Big Bang nucleosynthesis. Only after the first generation of stars explode as supernovae and achieve widespread metal pollution is metal line cooling possible. Thus, the star formation efficiency and the initial mass function (IMF) of Population III stars is likely to be set by the physical regime in which metal-free cooling can take place. In recent years, the cooling of metal-free gas in the first halos that are able to cool within a Hubble time $t_{\text{cool}} < t_{\text{H}}$, has come under intensive study (see Abel & Haiman 2000 for a recent review). Such halos have low virial temperatures, $T_{\text{vir}} < 10^4$ K; at these temperatures H₂ is formed via gas-phase processes such as $\text{H} + \text{e}^- \rightarrow \text{H}^- + \gamma$, followed by $\text{H}^- + \text{H} \rightarrow \text{H}_2 + \text{e}^-$. Detailed numerical simulations have shown convergence toward a regime $T \sim 200$ K, $n \sim 10^4 \text{ cm}^{-3}$, dictated by the thermodynamic properties of H₂ (Abel et al. 2000; Bromm et al. 2001a), which allows gas fragmentation into clumps of mass $10^2 - 10^3$ M_⊙.

However, as the first stars begin to shine, they emit photo-dissociating radiation in the Lyman–Werner bands (LW; 11.2–13.6 eV) to which the universe is optically thin, and further H₂ formation and cooling can be suppressed both by external (Haiman, Rees & Loeb 1997; Haiman, Abel & Rees 2000; Ciardi et al 2000; Machacek et al.

2001; Ricotti, Gnedin & Shull 2001a, 2001b) and internal (Omukai & Nishi 1999; Glover & Brand 2000) sources of UV radiation. This may be partially alleviated if X-rays with energies $\gtrsim 1$ keV (whose mean free path in a uniform IGM exceeds the Hubble length) can boost the free electron fraction, and thus the H₂ formation rate in cooling clumps (Haiman, Rees & Loeb 1996; Haiman, Abel & Rees 2000; Oh 2001); note that such effects are unlikely to be important in the low density environment of the IGM (Venkatesan, Giroux, & Shull, 2001). Alternatively, protogalactic shocks can produce substantial H₂ (Shapiro & Kang 1987; Ferrara 1998), or H₂ may be generated in front of HII regions or in relic HII regions (Ricotti, Gnedin & Shull 2001a, 2001b), or the optical depth in intergalactic H₂ may reduce the strength of the external dissociating radiation field (Ricotti, Gnedin & Shull 2000). However, while these effects may promote H₂ formation in the presence of an external UV background radiation field, they are unlikely to balance the strong internal feedback provided by stars within a galaxy: in the worst case scenario, only one star per halo can be formed (e.g., Madau & Rees 2001). It is therefore often believed that efficient and widespread star (and/or quasar black hole) formation capable of reionizing the universe must await the collapse of halos with $T_{\text{vir}} > 10^4$ K, or $M_{\text{halo}} > 10^8[(1+z)/11]^{-3/2}$ M_⊙ (Ostriker & Gnedin 1996, Haiman, Rees & Loeb 1997, Ciardi et

¹Hubble Fellow

al 2000, Abel & Haiman 2000, Ricotti, Gnedin & Shull 2001a, 2001b). These halos do not rely on the presence of H_2 molecules, since they can cool via recombination and collisional excitation of neutral atoms.

The goal of this paper is to critically examine the prevailing assumptions of efficient gas cooling and star formation in metal free halos with $T_{\text{vir}} > 10^4 \text{ K}$. To date, the details of gas cooling and chemistry in these halos have not been studied with the same care and attention devoted to lower mass halos. Since the majority of stars and/or quasars which reionized the universe, and polluted the intergalactic medium (IGM) with metals, are expected to form in such halos, it is important to study the evolution of the gas in these halos in detail.

It is generally taken for granted that $\text{Ly}\alpha$ cooling of neutral atomic hydrogen allows rapid contraction of gas until it becomes self-gravitating at the center of the potential well and fragments to form stars (ideas tracing back to Rees & Ostriker 1977; White & Rees 1978). However, it is also known that significant contraction is required for this fragmentation to result in stellar-mass fragments. If only $\text{Ly}\alpha$ cooling operates, the gas remains at a temperature of $\sim 10^4 \text{ K}$ due to the sharp cutoff in the (equilibrium) cooling function and the Jeans mass is exceedingly high, even at high densities: $M_J \approx 10^8 (T/10^4 \text{ K})^{3/2} (n/1 \text{ cm}^{-3})^{-1/2} M_\odot$. Even if the gas became self-gravitating, unless the gas can contract to extremely high densities, $n > 10^{12} \text{ cm}^{-3}$, fragmentation to lower Jeans masses $M \sim 100 M_\odot$ cannot proceed. However, the gas cannot cool to arbitrarily high densities, but eventually must form a rotationally supported disk; at the temperatures allowed by $\text{Ly}\alpha$ cooling, we shall show that the majority of such disks are locally gravitationally stable.

Thus, an additional coolant is needed to lower the gas temperature, both to ensure gravitational instability and to lower the Jeans mass by several orders of magnitude. In the absence of metals, H_2 formation and cooling is therefore still critical to star formation in $T_{\text{vir}} > 10^4 \text{ K}$ halos, and cannot be ignored. In this paper, we study H_2 formation in shock-heated gas, and show that a universal H_2 fraction of $x_{\text{H}_2} \approx 10^{-3}$ forms in gas that cools from an initial temperature of $T > 10^4 \text{ K}$. Similar behavior has already been noted in previous studies of pregalactic shocks (Shapiro & Kang 1987, Kang & Shapiro 1992). Here we study the non-equilibrium H_2 formation in the $T_{\text{vir}} > 10^4 \text{ K}$ halos of interest, examine the robustness of this mechanism to variations in density, temperature, and radiation field, and show that the asymptotic abundance can be understood in terms of timescale arguments. These arguments reveal that over a wide range of densities, the cooling gas follows a universal track in the (x_e, T) plane.

This paper is organized as follows. In §2, we study the equilibrium structure of isothermal disks embedded in dark matter halos, and show that H_2 cooling is needed to promote gravitational instability in most disks. In §3, we use semi-analytic methods and non-equilibrium chemistry to investigate H_2 formation and radiative cooling in halos with virial temperatures $T_{\text{vir}} > 10^4 \text{ K}$, and argue that the H_2 abundance builds up to a universal value of $x_{\text{H}_2} \approx 10^{-3}$ under most realistic conditions. In §4, we study the effects of H_2 destruction by internal and external sources of UV radiation and show that feedback processes are much

less efficient in $T_{\text{vir}} > 10^4 \text{ K}$ halos than in their smaller counterparts, primarily because in the larger halos, gas can be compressed to high densities by initial atomic line cooling. We also examine whether opacity and radiation pressure effects can halt the collapse or fragmentation. Although we conclude that this is unlikely, we argue that it could affect the efficiency of star formation. In §5, we summarize our conclusions and the implications of this work. In all numerical estimates, we assume a cold dark matter cosmology with a cosmological constant (ΛCDM) $(\Omega_m, \Omega_\Lambda, \Omega_b h^2, h, \sigma_{8h^{-1}}) = (0.3, 0.7, 0.019, 0.7, 1.0)$ (see, e.g., Bahcall et al. 1999 for a review of these choices).

2. DISK FORMATION AND GRAVITATIONAL INSTABILITY

Let us first consider the cooling and collapse of an initially spherical configuration of gas in a typical halo with $T_{\text{vir}} > 10^4 \text{ K}$. The discussion presented in this section serves two purposes: it will highlight the importance of H_2 molecules for the larger halos, and will also yield the physically appropriate range of density, temperature and ionization fractions under which to consider H_2 formation and cooling in later sections.

The well-known condition for runaway contraction of gas is $t_{\text{cool}} < t_{\text{dyn}} < t_{\text{sc}}$ (see Rees & Ostriker 1977), which is typically satisfied for hydrogen atomic line cooling. Since cooling due to $\text{Ly}\alpha$ has a very sharp cutoff at $T < 10^4 \text{ K}$, the cooling time is a very sensitive function of temperature, increasing rapidly by several orders of magnitude in a very narrow temperature range below $\sim 10^4 \text{ K}$ (Spitzer 1978). This is because the free electron fraction able to excite atomic line cooling drops very rapidly in this temperature range. Thus, the condition $t_{\text{cool}} < t_{\text{dyn}}$ implies that the collapse is nearly isothermal. If the gas cools below $\sim 10^4 \text{ K}$, the gas recombines, the cooling time rapidly increases until $t_{\text{cool}} > t_{\text{dyn}}$, and further contraction of the gas is close to adiabatic, with the gas heating up due to the contraction until the hydrogen atoms are collisionally re-ionized and the condition $t_{\text{cool}} < t_{\text{dyn}}$ is satisfied once again. In the absence of any other effects, this thermostatic mechanism would allow the gas in a $T_{\text{vir}} > 10^4 \text{ K}$ halo to cool and contract to arbitrarily high densities. In practice, however, the gas has some initial angular momentum, and must therefore eventually become rotationally supported. After a contraction by a factor of $\lambda^{-1} \sim 20$ in radius (where $\lambda \equiv J|E|^{1/2}/GM^{5/2}$ is the spin-parameter, and J , E , and M are the total angular momentum, energy and mass of the halo), this results in rotationally supported disk at the center of the halo (Mo, Mao & White 1998, hereafter MMW). It is possible that some fragmentation takes place as the gas collapses toward a disk, however, this is likely to be inefficient due to the slow growth of density fluctuations in a rapidly contracting medium (e.g., Kashlinsky & Rees 1983). We therefore assume that most fragmentation must take place in the disk itself. We shall show that if only atomic line cooling operates, the disk will be stable to fragmentation in the majority of cases. For fragmentation to proceed, an additional cooling channel (such as H_2) is required to allow cooling below $\sim 10^4 \text{ K}$.

For simplicity, we shall follow MMW, and assume that the gas settles to an isothermal, exponential disk, with gas temperature T_{gas} , embedded in a halo of virial temperature T_{vir} with a Navarro, Frenk & White (1997, here-

after NFW) dark matter density profile. We begin by listing the characteristic properties of such disks, which will be relevant for our later studies of H₂ formation and self-shielding. Let us assume that baryons make up the universal mass fraction Ω_b/Ω_m of the halo, of which some fraction f_d have collapsed into the disk, i.e. $M_{\text{disk}} = m_d M_{\text{halo}} = f_d (\Omega_b/\Omega_m) M_{\text{halo}}$. We also assume that the angular momentum of the disk J_d is some fraction j_d of the halo angular momentum J , i.e. $J_d = j_d J$. Henceforth, we shall assume that the specific angular momentum of the disk is similar to that of the halo, and thus $m_d = j_d$.

The assumption that the baryons preserve their specific angular momentum during collapse results in a good fit to the observed size distribution of galactic disks (Mo, Mao & White 1998). Detailed numerical simulations (Navarro & White 1993, Navarro & Steinmetz 2000) have not supported this simple model, but instead produced significantly smaller disks, due to the transfer of angular momentum from the gas to the dark matter during the highly inhomogeneous collapse. These simulations, however, also fail to produce the sizes and properties of observed galaxy-sized disks. Inclusion of suppression of cooling until late times (Weil, Eke & Efstathiou 1998) or supernovae feedback (Thacker & Couchman 2001) reduces the discrepancy, but the issue has yet to be conclusively resolved. We therefore simply extend successful semi-analytic models of disk formation at low redshift to higher redshift, and note that future numerical simulations of such halos may not in fact produce such disks.

The hydrogen number density at radius r and at vertical height z in an isothermal exponential disk of radial scale length R_d is given by (Spitzer 1942)

$$n(r, z) = n_o \exp\left(-\frac{2r}{R_d}\right) \operatorname{sech}^2\left(\frac{z}{\sqrt{2}z_o}\right), \quad (1)$$

where n_o is the central density, z_o is the vertical scale height of the disk at radius r ,

$$z_o = \frac{c_s}{(4\pi G \mu m_H n_o e^{-2r/R_d})^{1/2}} \quad (2)$$

c_s is the sound speed of the gas, and $\mu = 0.6$ is the mean molecular weight (we choose the definition of the disk scale length R_d to conform to the customary assumption that the surface density has an exponential profile: $\Sigma \propto \exp(-r/R_d)$). For a disk in a halo with spin parameter λ , if we assume the baryons conserve their specific angular momentum when they collapse, then the disk scale length is given by $R_d = 2^{-1/2} (j_d/m_d) \lambda r_{200} f_c^{-1/2} f_R \approx \frac{\lambda}{\sqrt{2}} r_{200}$, where $r_{200} \approx r_{\text{vir}}$ is the radius that encloses a mean interior mass density of $200 \rho_{\text{crit}}$, $f_c(c)$ and $f_R(\lambda, c, m_d, j_d)$ are dimensionless functions of order unity (MMW), and c is the dimensionless concentration parameter (NFW).

The central number density of the gas is obtained by setting $\int dz \int 2\pi r dr \mu m_p n(r, z) = M_{\text{disk}}$, which yields:

$$n_o \approx 3.2 \times 10^4 \left(\frac{f_d}{0.5}\right)^2 \left(\frac{T_{\text{gas}}}{8000 \text{ K}}\right)^{-1} \left(\frac{T_{\text{vir}}}{5 \times 10^4 \text{ K}}\right) \times \left(\frac{\lambda}{0.05}\right)^{-4} \left(\frac{1+z}{10}\right)^3 \text{ cm}^{-3} \quad (3)$$

²In another context, it was proposed that similarly high spin dark halos might be detected from their gravitational lensing signature (Jimenez et al. 1997).

When considering the characteristic densities for H₂ formation, it will be sufficient to consider densities at most an order of magnitude below the central density: gas with $n > 0.1 n_o$ comprises > 50% of the mass of the disk. Because hydrostatic support is only relevant in the vertical direction, as the gas cools the disk becomes thinner, with a reduced scale height $z_o \propto T_{\text{gas}}^{1/2}$. The vertical column density of gas as a function of radius is:

$$\begin{aligned} N_{\text{HI}}(r) &= \sqrt{2} n_o z_o \exp(-2r/R_d) \\ &= 3 \times 10^{23} \exp(-r/R_d) \left(\frac{T_{\text{vir}}}{5 \times 10^4 \text{ K}}\right)^{1/2} \times \\ &\quad \left(\frac{f_d}{0.5}\right) \left(\frac{\lambda}{0.05}\right)^{-2} \left(\frac{1+z}{10}\right)^{3/2} \text{ cm}^{-2} \end{aligned} \quad (4)$$

which is sufficient for self-shielding of the gas against both ionizing UV radiation and H₂ dissociating radiation in the LW bands to become important. Note that the column density is independent of the gas temperature.

We now consider the conditions for gravitational instability of the disk. In computing the rotation curve $V(r)$, we use the formalism of MMW, which takes into account the contraction induced in the inner regions of the halo by the cooling and formation of the disk. This is done by assuming the disk is assembled slowly and the angular momentum of dark matter particles is an adiabatic invariant (Blumenthal et al. 1986, Flores et al. 1993). For the disk to be locally gravitationally unstable despite the stabilizing effects of tidal shears and pressure forces, we require the Toomre parameter $Q < 1$, where (e.g. Binney & Tremaine 1987)

$$Q = \frac{c_s \kappa}{\pi G \Sigma}, \quad (5)$$

Σ is the disk surface mass density, and $\kappa = 1.41(V/r)(1 + d \ln V / d \ln r)^{1/2}$ is the epicyclic frequency. Regions in local disk galaxies where $Q > 1$ are observationally associated with very little star formation, indicating that the Toomre criterion is obeyed remarkably well (Kennicutt 1989). For our purposes, if $Q > 1$ everywhere throughout the disk, it is gravitationally stable and we assume no star formation takes place. Disks with high spin parameters have low surface densities and satisfy this criterion. For any given disk-halo system, we can calculate a critical spin parameter λ_{crit} for which the disk is marginally stable. Here we define λ_{crit} by the requirement that Q attains a minimum value of $Q = 1$ at least at one position in the disk. The fraction of halos that remain dark can therefore be found by integrating over the spin parameter distribution, $f_{\text{dark}} = \int_{\lambda_{\text{crit}}}^{\infty} p(\lambda) d\lambda$, where $p(\lambda)$ is given by

$$p(\lambda) d\lambda = \frac{1}{\sigma_{\lambda} (2\pi)^{1/2}} \exp\left(-\frac{\ln^2(\lambda/\bar{\lambda})}{2\sigma_{\lambda}^2}\right) \frac{d\lambda}{\lambda} \quad (6)$$

with $\bar{\lambda} = 0.05$ and $\sigma_{\lambda} = 0.5$ (e.g. Barnes & Efstathiou 1987, Warren et al. 1992).² Our use of the Toomre criterion to characterize gravitational instability depends on

the assumption that the disk is thin, $z_o \ll R_d$; in this case gravitational instability is insensitive to the vertical structure of the disk (Goldreich & Lynden-Bell 1965). The ratio of scale heights is given by

$$\frac{z_o}{R_d} = 1.5 \times 10^{-2} \left(\frac{T_{\text{gas}}}{8000 \text{ K}} \right) \left(\frac{T_{\text{vir}}}{5 \times 10^4 \text{ K}} \right)^{-1} \left(\frac{\lambda}{0.05} \right)^{-1} \left(\frac{f_d}{0.5} \right) \quad (7)$$

and thus $z_o \ll R_d$ is generally satisfied, except in low virial temperature halos where $T_{\text{vir}} \sim T_{\text{gas}}$.

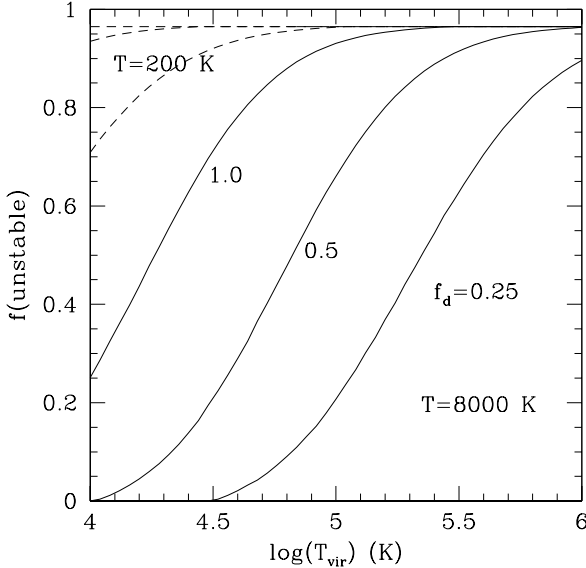


FIG. 1.— The fraction of disks that have sufficiently low spin to be locally gravitationally unstable at least at one radius, as a function of virial temperature T_{vir} of the halo. The computed curves are for $z=10$, but the results depend only very weakly on redshift. The solid and dashed curves assume gas temperatures of 8000 K (no H_2) and 200 K (effective H_2 cooling), respectively. For both temperatures, results are shown for three different disk mass-fractions, $f_d \equiv (M_{\text{disk}}/M_{\text{halo}})/(\Omega_b/\Omega_m) = 0.25, 0.5$, and 1. For $f_d = 0.25$, (as inferred for low redshift dwarfs), the majority of disks in low T_{vir} halos will be gravitationally stable.

From equation (5), it is clear that if the gas cools from $\sim 8000 \text{ K}$ to $\sim 200 \text{ K}$, this lowers by a factor of ~ 6 the critical surface density required for local gravitational instability. In Figure 1, we show the fraction of disk galaxies in halos with virial temperature T_{vir} that are gravitationally unstable at redshift $z = 10$, for different values of f_d . The most important result seen in this figure is that in the absence of H_2 , i.e., at a temperature of 8000 K, virtually all halos just above the threshold $T_{\text{vir}} \approx 10^4 \text{ K}$ harbor disks that are stable everywhere. Instability could be promoted if a large fraction, $f_d > 0.5$, of the baryons make up the disk, however, this is unlikely to be the case (see discussion below). Only in relatively large halos ($T_{\text{vir}} \gtrsim 10^5 \text{ K}$) would most disks be able to develop instabilities. This can be easily understood with a simple order of magnitude calculation assuming an exponential disk which reaches the asymptotic circular velocity on a disk scale length $R_d \approx \lambda r_{200}/\sqrt{2}$, which gives: $Q \approx 1.3(T_{\text{gas}}/8000 \text{ K})^{1/2}(T_{\text{vir}}/2 \times 10^4 \text{ K})^{-1/2}$ (a more detailed calculation gives a slightly lower value). Apart from a weak dependence on the redshift-dependent NFW concentration parameter c (at $z \sim 10$, we have $c \approx 5$ for halos with $T_{\text{vir}} \approx \text{few} \times 10^4 \text{ K}$), the Toomre parameter Q is in-

dependent of redshift for a halo of given T_{vir} and f_d , and thus the results of Figure 1 depend very weakly on the assumed redshift.

The figure also shows that decreasing the gas temperature significantly increases the fraction of unstable disks, particularly in low mass halos. To illustrate the effect of the gas temperature more clearly, we have computed the mass-weighted fraction of disks, embedded in all halos with $T_{\text{vir}} > 10^4 \text{ K}$, that are unstable to star formation:

$$\tilde{f}_{\text{unst}}(z) = \frac{\int_{M(T_{\text{vir}}=10^4 \text{ K}, z)}^{\infty} dM \frac{dN}{dM}(M, z) M f_{\text{unst}}(M, z)}{\int_{M(T_{\text{vir}}=10^4 \text{ K}, z)}^{\infty} dM \frac{dN}{dM}(M, z) M} \quad (8)$$

where the mass function $dN/dM(M, z)$ is obtained from standard Press-Schechter theory, and $f_{\text{unst}}(M, z)$ is the quantity computed in Figure 1. Thus, \tilde{f}_{unst} is the quantity directly relevant to most cosmogonic studies, representing the fraction of the total gas mass reservoir that will be available for star-formation. The resulting unstable fraction \tilde{f}_{unst} is shown as a function of redshift in Figure 2.

The figure reveals that depending on the value of f_d , the temperature drop caused by H_2 formation and cooling can significantly increase (by between one or two orders of magnitude) the mass fraction of collapsed halos that are able to form stars. If H_2 cooling does not proceed efficiently, then significant star formation, and therefore the epoch of reionization, has to likely await lower redshifts when still more massive ($T_{\text{vir}} \gg 10^4 \text{ K}$) halos collapse, or until the dispersal of metals from low-spin, star-forming halos sufficiently contaminates surrounding halos so that they can cool via metal lines.

Since $\Sigma \propto M_{\text{disk}}$, the question of whether a disk will be gravitationally unstable depends strongly on the mass fraction of baryons in the disk. As clearly revealed in Figures 1 and 2, if f_d is high, a larger fraction of disks will be gravitationally unstable. For simplicity, here we have assumed f_d to be a constant, but in reality it is likely to vary as a function of virial temperature. One might indeed expect that f_d is lower in halos with lower virial temperatures, owing to the increased efficiency of feedback processes in shallow potential wells. This would accentuate the trend for disks in low mass halos to be gravitationally stable. For reference, $f_d \approx 0.4$ yields good agreement with the observed sizes of disks and rotation curves over a wide range of circular velocities (MMW). More appropriately for our purposes, van den Bosch, Burkert & Swaters (2001) fitted angular momentum models to a sample of observed low-mass disk galaxies with $V_{\text{circ}} \sim 75 - 150 \text{ km s}^{-1}$ (still somewhat more massive than the galaxies we are considering); they found best-fit mass fractions to be considerably lower than the universal baryonic fraction, with a mean value of $f_d \sim 30\%$. Interestingly, they find that although disks form out of only a small fraction of the available baryons, they nonetheless draw most of the available angular momentum. If disks formed only out of low angular momentum baryons in the halo, they would be exceedingly compact, obviating our conclusions.

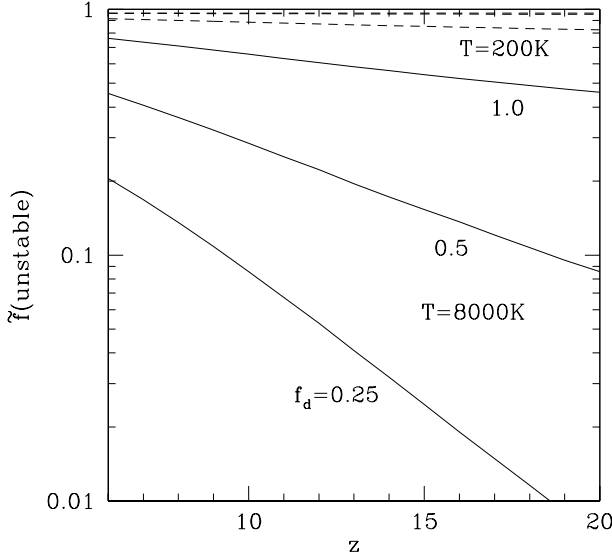


FIG. 2.— Mass-weighted unstable disk fraction as a function of redshift, as given by equation (8). At every redshift, the mass fraction in Toomre unstable disks have been summed over all halos with $T_{\text{vir}} \geq 10^4 \text{K}$. Thus, f_{unst} represents the fraction of the total gas mass reservoir that will be available for star-formation in all collapsed halos. The curves are labeled as in Figure 1. If H_2 cooling is ineffective, then the gas fraction available for star formation in collapsed halos is considerably lower.

It is not clear what direction f_d should take towards higher redshift. While Ly α cooling is likely to be more effective at the higher densities, typical masses and virial temperatures are even lower than those considered by van den Bosch et al. (2001), metal line cooling is absent, and a possibly top-heavy IMF results in more intense ionizing radiation (Bromm, Kudritzki & Loeb 2001) once internal star formation is underway and is also more likely to produce hypernovae explosions (Heger & Woosley 2001). All of these effects should suppress gas cooling efficiencies and lower f_d . If $f_d \sim 30\%$, as at low redshift, then from Figure 2, only \sim few% of the gas in disks will be available for star formation at redshifts $z > 10$.

In summary, our results in this section underscore the need for H_2 formation in order for most disks to be unstable. In the next section, we will show that a significant amount of H_2 is indeed expected to form in virtually all realistic cases; while in section §4 we consider the feedback processes which might suppress H_2 formation and cooling.

3. CHEMISTRY AND GAS COOLING IN $T_{\text{VIR}} > 10^4 \text{K}$ HALOS

In this section, we follow the coupled chemical and thermal evolution of a single fluid element when no UV flux is present. We find that in gas cooling from above $\sim 10^4 \text{K}$, H_2 forms with a fixed abundance $x_{\text{H}_2} \sim 10^{-3}$, which is *not* its equilibrium value, under a wide variety of initial conditions. We obtain a quantitative explanation for this value and the reason for the universality of this abundance. Readers not interested in the technical details may skip the rest of this section. We defer discussion of the case where UV flux is present to §4.

It is not immediately obvious that H_2 can form in gas

cooling down from $T_{\text{vir}} > 10^4 \text{K}$, since destruction of H_2 by charge exchange and collisional dissociation is very effective in gas at temperatures $T > 5000 \text{K}$. There is a trough in the equilibrium cooling curve between $\sim 8000 \text{K}$ (when Ly α cooling is effective) and $\sim 3000 \text{K}$ (when H_2 cooling becomes effective), and it is possible that gas could cool to $\sim 5000 \text{K}$ and recombine before sufficient H_2 forms to cool the gas to lower temperatures, hanging up in the valley between the peaks of the two cooling curves (e.g., see figure 12 of Barkana & Loeb 2001).

The chemistry and cooling of primordial gas cooling from above 10^4K has previously been considered by integrating the coupled rate equations in the limit of steady state shock waves (Shapiro & Kang 1987, Kang & Shapiro 1992, hereafter KS). These authors find that H_2 formation is indeed possible and that gas can cool continuously to $\sim 200 \text{K}$, the limiting temperature at which H_2 molecules comes into local thermodynamic equilibrium (LTE), and cooling is no longer effective. The efficacy of H_2 formation is due to the large non-equilibrium abundance of electrons in gas cooling from above $T > 10^4 \text{K}$; the gas cools and forms H_2 faster than it recombines. Shapiro & Kang (1987) and subsequent authors have noted that H_2 tends to form with an asymptotic abundance of $\sim 10^{-3}$ over a wide range of initial conditions. We confirm this result, explore the process of H_2 formation semi-analytically, and demonstrate how this asymptotic abundance can be understood in terms of timescale arguments. Similar results have been obtained recently by Susa et al. (1998).

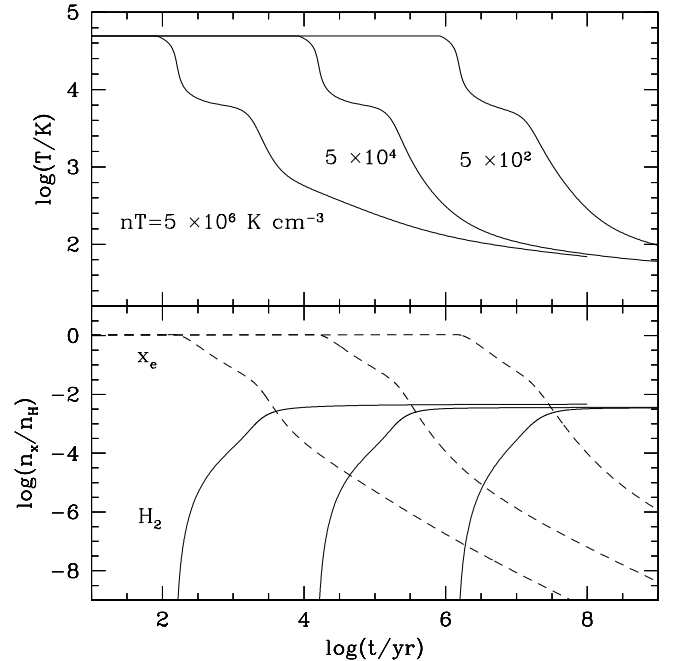


FIG. 3.— The temperature (top panel), H_2 and electron abundance (bottom panel) evolution as a function of time for a parcel of gas cooling isobarically from $T = 5 \times 10^4 \text{K}$, with no dissociating UV flux. Regardless of the density of the gas, the H_2 abundance asymptotes to a universal fraction $x_{\text{H}_2} \sim 10^{-3}$. The evolution of the gas is self-similar, with timescales scaling as $1/n$, except at high gas densities $n > 10^4 \text{cm}^{-3}$, when LTE effects become important. Thus, for the $nT=5 \times 10^6 \text{Kcm}^{-3}$ curve, the temperature evolution deviates from self-similarity at low temperatures (high densities). See text for details.

3.1. A universal H_2 abundance

Here, we show that over a wide range of initial conditions, H_2 forms in cooling gas with a universal abundance $x_{\text{H}_2} \sim 10^{-3}$ which is *not* the equilibrium value.

We begin by using a full non-equilibrium chemistry code to solve the rate equations for gas cooling from above 10^4 K. The code solves the coupled set of stiff equations using the Livermore stiff solver LSODAR, assuming primordial abundances and starting from the initial conditions $T_{\text{gas}} = T_{\text{vir}}$ and assuming equilibrium ionization fractions at T_{vir} as the initial condition (for $T_{\text{vir}} = 5 \times 10^4$ K, $x_e = 1$). The reaction network we use in our calculations is given in a Table in the Appendix. The rates are identical to those used in Haiman, Rees & Loeb (1996), unless marked otherwise. In Figure 3, we show results from the code for gas cooling isobarically (the results for isochoric cooling are very similar). For a wide range of initial densities, the H_2 abundance asymptotes to a universal value $x_{\text{H}_2} \sim 10^{-3}$. We also obtain this universal H_2 abundance for any starting temperature $T_{\text{vir}} > 1.2 \times 10^4$ K.

Does this universal abundance simply reflect the equilibrium abundance of H_2 at low temperatures? The equilibrium abundance of n_{H_-} is given by:

$$\begin{aligned} n_{\text{H}_-} &= \frac{k_9 n_{\text{H}} n_e + k_{14} n_{\text{H}_2} n_e}{(k_{10} + k_{20}) n_{\text{H}} + (k_{13} + k_{21}) n_{\text{H}^+} + k_{19} n_e} \\ &\approx \frac{n_{\text{H}} n_e - k_9}{n_{\text{H}} k_{10} + n_{\text{H}^+} k_{13}} \approx \frac{n_e - k_9}{k_{10}} \end{aligned} \quad (9)$$

The various approximations indicate the most important terms, which we have identified directly from the non-equilibrium chemistry code. The last approximation holds for $x_e < 0.03$, when the H_2 abundance rises rapidly and approaches its asymptotic value. The equilibrium abundance of H_2 is then given by:

$$\begin{aligned} n_{\text{H}_2} &= \frac{k_{10} n_{\text{H}} n_{\text{H}^-}}{(k_{14} + k_{17} + k_{18}) n_{\text{H}^+} + k_{15} n_{\text{H}}} \\ &\approx \frac{k_{10} n_{\text{H}} n_{\text{H}^-}}{k_{17} n_{\text{H}^+}} \approx \frac{k_9 n_{\text{H}}}{k_{17}} \end{aligned} \quad (10)$$

where again the last approximation holds for $x_e < 0.03$. Note that in this regime $x_{\text{H}_2} \approx k_9/k_{17}$ is independent of density or ionization fraction and depends only on the temperature. It is interesting to note that collisional dissociation of H_2 , given by $\text{H}_2 + \text{H} \rightarrow 3\text{H}$, is unimportant in this regime, contrary to previous assumptions (e.g. Omukai 2001). Instead, the destruction of H_2 is governed primarily by the charge-exchange reaction, $\text{H}_2 + \text{H}^+ \rightarrow \text{H}_2^+ + \text{H}$; when the gas is fully ionized, H_2 formation is strongly suppressed. This is why recombination and H_2 formation both initially proceed on the same timescale in Figure 3.

We now use these expressions to check if H_2 remains in equilibrium throughout the cooling process. In the lower panel of Figure 4, we plot the equilibrium abundance of H_2 (as given by the full, rather than reduced expressions for equations 9 and 10), against the actual computed value of the H_2 abundance given by the chemistry code. Initially, the H_2 abundance follows the equilibrium value. However, as the gas cools to lower temperatures $T < 3700$ K, it deviates sharply from equilibrium: the H_2 abundance asymptotes to the value $x_{\text{H}_2}^{\text{asym}} \sim 10^{-3}$, while the equilibrium

value continues to rise. Thus, the universal abundance does *not* reflect the equilibrium abundance of H_2 at low temperatures, which is significantly higher.

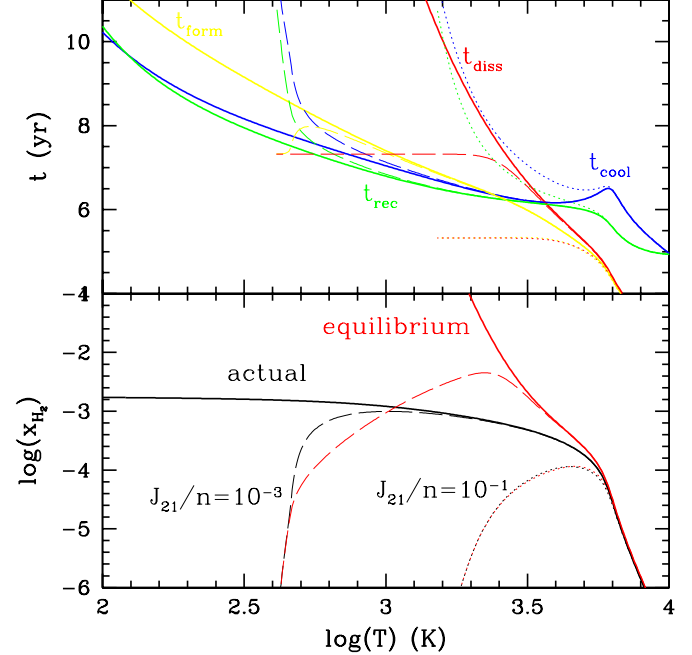


FIG. 4.— The evolution of the H_2 abundance as a function of temperature, starting from $T > 10^4$ K. Solid lines indicate the no flux case; the dashed lines ($J_{21}/n = 10^{-3}$) and dotted lines ($J_{21}/n = 10^{-1}$) illustrate the case when a dissociating UV flux is present (see section §4.2 for details; J_{21} has units of $10^{-21} \text{ erg s}^{-1} \text{ cm}^{-2} \text{ Hz}^{-1} \text{ sr}^{-1}$, and n has units of cm^{-3}). The bottom panel shows the equilibrium (as given by equation (10) and the actual (computed by the full non-equilibrium chemistry code)) H_2 abundance, while the top panel shows the timescales for H_2 formation t_{form} , dissociation t_{diss} , gas cooling t_{cool} and electron recombination t_{rec} . Initially at high temperatures the H_2 formation and destruction timescales are short compared to $t_{\text{sys}} = \min(t_{\text{rec}}, t_{\text{cool}})$, and the H_2 abundance is in equilibrium, $t_{\text{form}} = t_{\text{diss}}$. Once $t_{\text{diss}}, t_{\text{form}} > t_{\text{sys}}$ at $T \sim 3700$ K, the H_2 abundance falls out of equilibrium, and “freezes out” at $x_{\text{H}_2} \sim 10^{-3}$. When a dissociating UV flux is present, t_{diss} asymptotes to a fixed value, instead of rising exponentially. Eventually, t_{diss} becomes the shortest timescale in the problem. At this point, the H_2 abundance falls back into equilibrium, and decreases rapidly.

3.2. Why is $x_{\text{H}_2} \sim 10^{-3}$?

Here we show that the asymptotic abundance of $x_{\text{H}_2} \sim 10^{-3}$ may be *quantitatively* understood as a result of freeze-out processes.

The H_2 will no longer evolve (“freeze-out”) if the H_2 formation and dissociation timescales are much longer than any other characteristic timescale in the system:

$$t_{\text{form}}, t_{\text{diss}} \gg t_{\text{rec}}, t_{\text{cool}} \quad (11)$$

where $t_{\text{form}} \equiv \frac{n_{\text{H}_2}}{n_{\text{form}}} \approx \frac{x_{\text{H}_2}}{x_e n k_9(T)}$ is the H_2 formation time, $t_{\text{diss}} \equiv \frac{n_{\text{H}_2}}{n_{\text{diss}}} \approx \frac{1}{k_{17}(T) n x_e}$ is the H_2 dissociation time, t_{cool} is the cooling time, and $t_{\text{rec}} \equiv \frac{1}{x_e n k_4}$ is the electron recombination time. The cooling and recombination timescales regulate the temperature T and the ionization fraction x_e , which in turn affect the H_2 abundance.

We plot these timescales, as extracted from the full non-equilibrium calculation, in the top panel of Fig. (4). As

the gas cools, the dissociation timescale t_{diss} grows rapidly and the gas falls out of equilibrium. Shortly thereafter, t_{form} exceeds $t_{\text{rec}}, t_{\text{cool}}$, and the H_2 abundance freezes out.

The rapid growth of t_{diss} is easy to understand. The rates for collisional dissociation k_{15} and charge exchange k_{17} (H_2 dissociation is primarily due to the latter) decrease exponentially as the temperature drops. On other hand, all other timescales $t_{\text{form}}, t_{\text{cool}}, t_{\text{rec}}$ have only a power-law temperature dependence. Therefore as the gas cools the dissociation time rises exponentially and rapidly becomes much longer than all other timescales.

Let us denote the temperature at which $t_{\text{diss}} > t_{\text{rec}}, t_{\text{cool}}$ as T_{freeze} . Since t_{diss} depends much more sensitively on temperature than $t_{\text{rec}}, t_{\text{cool}}$, it exceeds them in very close succession. We can simply solve $t_{\text{diss}} = t_{\text{rec}}$ to obtain:

$$k_{17}(T) = k_4(T) \Rightarrow T_{\text{freeze}} = 3700\text{K} \quad (12)$$

Up to this point, the H_2 abundance is in equilibrium. The equilibrium value of H_2 at T_{freeze} is:

$$x_{\text{H}_2}^{\text{freeze}} \approx k_9(T_{\text{freeze}})/k_{17}(T_{\text{freeze}}) \approx 2 \times 10^{-3} \quad (13)$$

which is in excellent agreement with the calculated value, $\sim 1 - 2 \times 10^{-3}$.

For $T < T_{\text{freeze}}$, $t_{\text{diss}} \gg t_{\text{form}}$, due to exponential temperature dependence of t_{diss} discussed above. Thus, H_2 formation is more rapid than H_2 destruction and $x_{\text{H}_2} \geq x_{\text{H}_2}^{\text{asymp}}$. However, if $t_{\text{form}} > t_{\text{rec}}, t_{\text{cool}}$ for $T < T_{\text{freeze}}$, then the H_2 abundance will freeze out. Since $t_{\text{form}} \approx t_{\text{diss}} \approx t_{\text{rec}}$ at T_{freeze} , we can write:

$$\frac{t_{\text{form}}}{t_{\text{rec}}} = \left(\frac{x_{\text{H}_2}}{x_{\text{H}_2}^{\text{asymp}}} \right) \left(\frac{T}{T_{\text{freeze}}} \right)^{-1.7} \quad (14)$$

Since $x_{\text{H}_2} \geq x_{\text{H}_2}^{\text{asymp}}$, we conclude that $t_{\text{form}} > t_{\text{rec}}$, for $T < T_{\text{freeze}}$. Similarly, we have:

$$\frac{t_{\text{form}}}{t_{\text{cool}}} \propto x_{\text{H}_2} T^2 x_e^{-1} \quad (15)$$

(where we have assumed $\Lambda_{\text{H}_2} \propto T^4$, a good approximation for $T < 3000\text{K}$). As before, $x_{\text{H}_2} \geq x_{\text{H}_2}^{\text{asymp}}$, so the minimum value of $t_{\text{form}}/t_{\text{diss}}$ is given by $x_{\text{H}_2} = x_{\text{H}_2}^{\text{asymp}}$. If we evolve the rate equations at fixed $x_{\text{H}_2} = x_{\text{H}_2}^{\text{asymp}}$, the quantity T^2/x_e increases with time. Thus, $t_{\text{form}} > t_{\text{cool}}$ for $T < T_{\text{freeze}}$.

Since $t_{\text{diss}}, t_{\text{form}} \gg t_{\text{rec}}, t_{\text{cool}}$, the conditions for freeze-out are satisfied. The H_2 follows its equilibrium abundance until $T_{\text{freeze}} = 3700\text{K}$, whereupon it freezes out. Our simple estimate from timescale arguments (12), (13) for T_{freeze} and x_{asymp} agree quantitatively with the full non-equilibrium calculation shown in Fig (4). This gives us confidence that we understand the dominant physical processes at work.

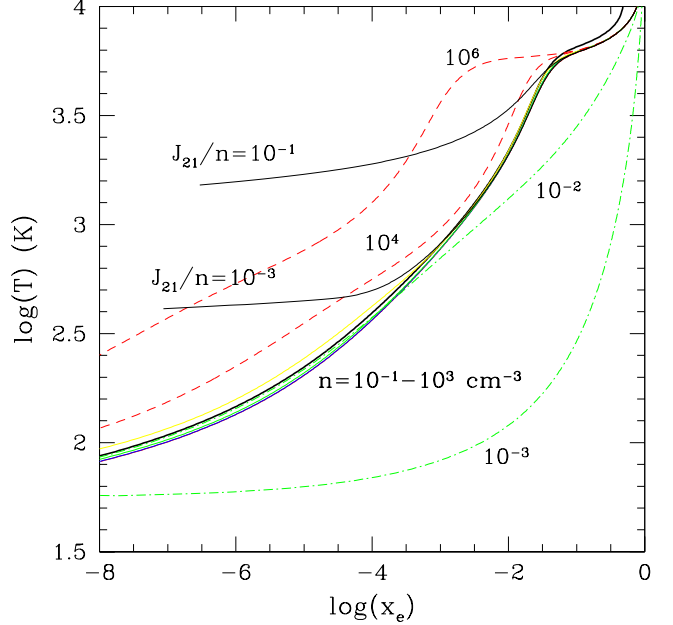


FIG. 5.— The evolution of the gas temperature against the ionization fraction. The gas always cools along the same evolutionary pathway (shown in bold), regardless of whether it cools isobarically or isochorically, as long as the density stays within the limits $n \approx 0.1 - 10^3 \text{ cm}^{-3}$. Self-similarity is broken at low and high density: at low densities (dot-dashed lines) cooling off the CMB becomes important (the tracks here are for gas at $z=20$); at high densities $n > 10^3 \text{ cm}^{-3}$ (dashed lines), the H_2 coolant reaches LTE and cooling becomes less efficient. Also shown are the tracks when a dissociating UV flux is present (see section 4), labelled by the value of J_{21}/n . The gas follows the universal track until H_2 is dissociated and then recombines at constant temperature.

3.3. Self-similarity

All of the relevant timescales in this problem scale as $\propto \frac{1}{n}$. Thus, their ratio is independent of density, and the evolution of the gas should be 'self-similar'. There are three important variables controlling the evolution of the system: (T, x_e, n) . Since the ratio of the timescales controlling (T, x_e) are independent of n , the evolution of the gas in the (x_e, T) plane should be independent of n (note that self-similarity would *not* be observed if x_e or T were plotted against tn , as in e.g. Shapiro & Kang (1987), since in this case there is one 'hidden variable' which is missing from the plots).

In Figure 5, we plot T against x_e as obtained by running the full chemistry code and find that indeed the evolution of the gas is self-similar. This is subject to the following caveats: (i) at low density and high redshift, Compton cooling of the gas becomes effective; i.e., the gas cools faster by Compton cooling than it recombines. Compton cooling is important in the regime $t_{\text{cool}}^{\text{Compton}} < t_{\text{rec}}$, i.e. when

$$n < 8 \times 10^{-3} \left(\frac{T}{8000 \text{ K}} \right)^{0.7} \left(\frac{1+z}{20} \right)^4 \text{ cm}^{-3} \quad (16)$$

Since the Compton cooling timescale is independent of density, the self-similar scaling is broken in the low density regime, and the gas cooling rate is enhanced relative to the recombination rate (see the dot-dashed curves in Figure 5). (ii) At high densities $n > 10^4 \text{ cm}^{-3}$, the H_2 cooling

rate $\propto n$ instead of $\propto n^2$, as the H_2 levels reach LTE (Galli & Palla 1998). Thus, the cooling time becomes independent of density, rather than $t_{\text{cool}} \propto \frac{1}{n}$, again breaking the self-similar scaling. In this case, the recombination rate is enhanced relative to the gas cooling rate (see dashed curves in Figure 5). However, between these two bounds the track in (x_e, T) space followed by the cooling gas (solid lines in Figure 5) is independent of the density and indeed whether the gas cools isochorically or isobarically.

This convenient fact allows for considerable ease when estimating timescales, since it collapses a system of two variables into one variable, and allows one to 'evolve' a system without integrating the full rate equations. For the convenience of the reader we provide a fitting formula to this track:

$$\log_{10}(T) = 10^{a_0 + a_1 x + a_2 x^2 + a_3 x^3 + a_4 x^4}; \quad x_e > 10^{-2}$$

$$\log_{10}(T) = b_0 + b_1 x + b_2 x^2 + b_3 x^3 + b_4 x^4; \quad x_e \leq 10^{-2}$$

where $x \equiv \log_{10}(x_e)$ and $a_0 = 0.683, a_1 = 0.379, a_2 = 0.522, a_3 = 0.299, a_4 = 5.67 \times 10^{-2}$; and $b_0 = 4.56, b_1 = 0.789, b_2 = 9.73 \times 10^{-2}, b_3 = 6.74 \times 10^{-3}$, and $b_4 = 2.21 \times 10^{-4}$. This fit is valid to within $\sim 0.5\%$ in dex over the range of scales shown in Figure 5.

The cooling path followed by the gas is also independent of the initial temperature of the gas, as long as the initial ionization fraction is somewhat greater than its value at freeze-out, $x_e \approx 2.4 \times 10^{-2}$, which translates into $T > 1.2 \times 10^4$ K. This is because the gas recombines at nearly constant temperature $T \sim 9000$ K, and thus loses memory of its initial temperature and ionization fraction (see the plateau in temperature in Fig. 3).

We can use the self-similar scaling between temperature and ionization fraction to estimate the timescale on which the H_2 abundance reaches its peak value. While the temperature as a function of time is difficult to estimate, the ionization fraction as a function of time is straightforward. It is given by:

$$x_e(t) \approx \frac{x_o}{1 + t/t_{\text{rec},o}} \quad (17)$$

where $x_o = 1$ is the initial electron abundance and $t_{\text{rec},o} = 1/k_4 x_o n_{\text{H}} = 5.6 \times 10^4 \left(\frac{n_{\text{g}}}{1 \text{cm}^{-3}}\right)^{-1}$ yr (at 8000 K). At the freeze-out temperature $T_{\text{freeze}} = 3700$ K, the ionization fraction is $x_e \approx 2.4 \times 10^{-2}$. Thus, H_2 builds up to its peak abundance on an approximate timescale $t \approx 2 \times 10^6 \left(\frac{n_{\text{g}}}{1 \text{cm}^{-3}}\right)^{-1}$ yr.

For runaway collapse and fragmentation, we require $t_{\text{cool}} < t_{\text{dyn}}$. For $x_{\text{H}_2} \sim 10^{-3}$, we have:

$$\frac{t_{\text{cool}}}{t_{\text{dyn}}} = 0.22 \left(\frac{n_{\text{g}}}{1 \text{cm}^{-3}}\right)^{-1/2} \left(\frac{T}{10^3 \text{K}}\right)^{-3} \quad (18)$$

where we have assumed $\Lambda_{\text{H}_2} \propto T^4$, a good approximation for $T < 3000$ K. In $T_{\text{vir}} > 10^4$ K halos, gas will always contract via atomic cooling to high densities such that $t_{\text{cool}} < t_{\text{dyn}}$. This is in contrast to $T_{\text{vir}} < 10^4$ K halos, where only H_2 cooling is available, and only the high-density gas at the center of the halo can fragment.

In summary, we find that the universal abundance $x_{\text{H}_2} \sim 10^{-3}$ is the result of a "freeze-out" process. The H_2 abundance follows its equilibrium value until the freeze-out temperature $T_{\text{freeze}} \approx 3700$ K, at which point the H_2

formation and destruction timescales exceed the timescales on which the system cools and recombines. At this temperature, the H_2 abundance freezes out and stops evolving. In the absence of dissociating flux, H_2 formation and destruction timescales, as well as gas cooling and recombination timescales, all depend on collisional processes and scale as $\propto 1/n$. Hence, their ratio is independent of density and the behavior of the gas is self-similar.

4. FEEDBACK AND SELF-REGULATING STAR FORMATION

In the previous section, we have seen that in the absence of feedback, H_2 always forms with an abundance of $x_{\text{H}_2}^{\text{asymp}} \sim 10^{-3}$. In this section, we consider effects that can, in principle, modify this conclusion. There are three principal feedback effects that can potentially inhibit gas cooling and star formation in a disk: (i) UV radiation and supernovae explosions heating the disk back up to $\sim 10^4$ K, rendering the disk Toomre stable once again (ii) external dissociating UV radiation preventing H_2 formation and cooling (iii) internal dissociating UV radiation. In addition, we consider (iv) Ly α photon trapping, which may cause the gas to become radiation pressure dominated and prevent contraction to high densities. We discuss each of these effects in turn.

4.1. Gas heating and photoionization

Our assumption of an isothermal disk is obviously an idealization; both thermal instability and feedback from star formation implies that the gas should develop a multi-phase structure. Nonetheless, as we have seen in §2, for low mass disks to remain Toomre unstable, the dominant thermal phase must be cold ($T \sim 200$ K). It might be a concern that photoionizing radiation from forming stars could heat the disk back up to $T \sim 10^4$ K, stabilizing the disk once again. The production rate of ionizing photons necessary for most of the disk to be photoionized is:

$$\begin{aligned} \dot{N}_{\text{ion}} &\approx \alpha_B \int n_e^2 dV \\ &= 10^{56} \left(\frac{f_d}{0.5}\right)^3 \left(\frac{T_{\text{gas}}}{10^4 \text{K}}\right)^{-1.7} \left(\frac{T_{\text{vir}}}{5 \times 10^4 \text{K}}\right)^{5/2} \\ &\quad \left(\frac{\lambda}{0.05}\right)^{-4} \left(\frac{1+z}{10}\right)^{1.5} \text{ photons s}^{-1} \end{aligned} \quad (19)$$

For a zero-metallicity Salpeter IMF with $0.1 < M_*/M_{\odot} < 100$ when the lifetime of the starburst is $\tau \sim 10^6$ yrs, the stellar ionizing photon production rate is $\dot{N}_{\text{ion}} \approx 10^{53} \left(\frac{M_{*,\text{tot}}}{10^6 M_{\odot}}\right)$ photons s $^{-1}$, where $M_{*,\text{tot}}$ is the total mass in stars (Tumlinson & Shull 2000). The entire disk gas mass would be converted into stars before this stabilizing mechanism becomes important. If the stellar IMF consists wholly of supermassive stars $M > 100 M_{\odot}$, the ionizing photon production efficiency is an order of magnitude greater (Bromm et al 2001c), and this feedback mechanism may be marginally important. A likely much more important feedback mechanism could be supernova explosions, which can heat the gas to higher temperatures, and unbind it from the disk. A detailed quantitative understanding of supernovae feedback is still elusive (for recent progress see Efstathiou 2000, Mac-Low & Ferrara 1999). We merely

note that the effect of supernova explosions is devastating for low mass halos, but it becomes progressively less severe for $T > 10^4$ K halos. The potential wells are deeper, the gas contracts to the center of halos to yield higher binding energies, and SNe are surrounded by a denser ambient medium, which can radiate away the energy of the explosion more efficiently.

Another potential feedback process is production of secondary electrons by X-ray sources. This could be an important effect if the first light sources were mini-quasars (Haiman, Abel & Rees 2000), or high-redshift supernovae were an important source of X-rays (Oh 2001). This delays H_2 formation and cooling, since the secondary electrons produced increase the rate of H_2 destruction by charge exchange processes (Kang & Shapiro 1992). As the gas gradually cools and recombines, the electron fraction falls and H_2 production can proceed, unless the rate of X-ray heating can balance gas cooling at $\sim 10^4$ K to achieve stable thermal equilibrium.

4.2. Photodissociation by an external UV field

Here we consider the effects of an external photodissociating UV radiation field. We show that H_2 formation and cooling depends primarily on a single parameter, J_{21}/n , which controls the peak H_2 abundance and thus the minimum temperature T_{\min} a parcel of gas can cool to. The value of J_{21}/n is significantly smaller in $T_{\text{vir}} > 10^4$ K halos: atomic cooling allows the gas to contract to much higher initial densities. Thus, the effects of an external UV radiation field are much less important, even if the gas does not self-shield. Throughout the rest of this paper J_{21}/n is implicitly given in units of $10^{-21}\text{erg s}^{-1}\text{cm Hz}^{-1}\text{sr}^{-1}$.

4.2.1. The importance of J_{21}/n

The timescale for photodissociation is given by (Draine & Bertoldi 1996):

$$t_{\text{diss}} = \frac{1}{k_{\text{diss}}} = 2.1 \times 10^4 J_{21}^{-1} f_{\text{shield}}^{-1} \text{yr} \quad (20)$$

where J_{21} is the average flux in the LW bands in units of $10^{-21}\text{erg s}^{-1}\text{cm}^{-2}\text{Hz}^{-1}\text{sr}^{-1}$, and the factor f_{shield} takes into account the effects of H_2 self-shielding for a static clump of gas. For now we simply set $f_{\text{shield}} = 1$; we will consider the effects of self-shielding later, at the end of this section. Unlike all the other timescales previously considered, t_{diss} is independent of density. Photodissociation thus breaks the self-similarity of the no-flux case, where all timescales scaled as $1/n$. Since $t_i/t_{\text{diss}} \propto J_{21}/n$ (where $i = \text{rec, cool, form}$), the cooling history of the gas should depend only on the parameter J_{21}/n . We show this in detail below.

Dependence of $x_{H_2}^{\text{peak}}$ on J_{21}/n As the gas cools and recombines from above 10^4 K, it initially follows the no-flux case, where dissociation by charge exchange is the shortest timescale in the problem. However, as the temperature drops, photodissociation will take over. From $t_{\text{diss}}^{\text{photo}} = t_{\text{diss}}^{\text{charge-exchange}}$, this takes place when:

$$\left(\frac{J_{21}}{n}\right) \approx 1.5 \times 10^{-2} \exp\left[-\frac{3700\text{K}}{\text{T}}\right] \left(\frac{x_e}{2.4 \times 10^{-2}}\right) \quad (21)$$

At late times (low T and x_e), LW dissociation will always dominate H_2 destruction. Instead of rising exponentially as the temperature drops, the H_2 dissociation time remains constant (provided self-shielding is unimportant), becoming the shortest timescale in the problem as $t_{\text{cool}}, t_{\text{rec}}$ rise. Thus, the H_2 abundance rises to a peak value before steadily declining once $t > t_{\text{diss}}$.

The peak abundance of H_2 can be estimated as follows. The cooling gas follows the no flux evolution along the universal track until the condition in equation (21) is satisfied at some branch-out temperature T_{bo} . Observe that equation (21) is a function of only the temperature, since $x_e(T)$ is given by the fit to the universal cooling track. There are two possibilities: (1) $T_{\text{bo}} < T_{\text{freeze}}$, i.e. $J_{21}/n < 1.5 \times 10^{-2}$. In this case, $x_{H_2}^{\text{peak}} \sim x_{H_2}^{\text{asymp}} \sim 10^{-3}$. The H_2 abundance reaches the asymptotic freeze-out value and falls out of equilibrium, until $t_{\text{rec}}, t_{\text{cool}}$ increase sufficiently that $t_{\text{diss}} < t_{\text{rec}}, t_{\text{cool}}$. At this point, H_2 falls back into equilibrium and its abundance steadily decreases. (2) $T_{\text{bo}} > T_{\text{freeze}}$, i.e., $J_{21}/n > 1.5 \times 10^{-2}$. In this case, photodissociation becomes important before freeze-out can occur. H_2 is always in equilibrium, and we can compute the peak abundance simply from the equilibrium abundance of H_2 at T_{bo} , i.e. $x_{H_2}(x_e(T_{\text{bo}}), T_{\text{bo}})$.

These expectations are clearly borne out in runs with the full non-equilibrium chemistry code. In Figure (4), we plot the various timescales discussed above and the H_2 abundance as a function of temperature. We consider two different flux levels: $J_{21}/n = 10^{-1}$ (dotted lines) and $J_{21}/n = 10^{-3}$ (dashed lines), which bracket the critical value of $J_{21}/n = 1.5 \times 10^{-2}$. For $J_{21}/n = 10^{-1}$, the H_2 abundance never reaches freeze out but always follows the equilibrium value, whereas for $J_{21}/n = 10^{-3}$, the gas reaches the freeze-out value of $x_{H_2} \sim 10^{-3}$ and falls out of equilibrium, only to fall back into equilibrium when $t_{\text{diss}} = \min(t_{\text{rec}}, t_{\text{cool}})$. The H_2 abundance declines rapidly thereafter. In Figure 5, we see that the cooling gas follows the universal track until an abrupt transition takes place, corresponding to $t_{\text{diss}} = \min(t_{\text{rec}}, t_{\text{cool}})$, at which point the gas stops cooling and recombines at constant temperature.

Dependence of T_{\min} on J_{21}/n The results above suggest that the minimum temperature T_{\min} the gas can cool to depends on J_{21}/n . We have verified this by running the full chemistry code for a parcel of gas at different densities and under different flux levels, assuming isobaric cooling (the result is independent of the time the gas has available to cool t_H as long as $t_{\text{diss}} < t_H$. If $t_{\text{diss}} > t_H$, then photodissociation is in any case unimportant). In Figure 6, we plot the minimum temperature a parcel of gas cools down to, T_{\min} against J_{21}/n . Where the cooling of the gas is in the self-similar regime $n \sim 10^{-1} - 10^4\text{cm}^{-3}$, the curves lie on top of one another regardless of the absolute values of J_{21}, n , confirming that T_{\min} is a function only of one variable J_{21}/n . When $n > 10^4\text{cm}^{-3}$ then as before this scaling behavior is broken: the cooling time becomes independent of density and the gas cools less efficiently. In particular T_{\min} is no longer a function of J_{21}/n but just J_{21} (see dashed line). We explore this regime in more detail in §4.3.

We can compute T_{\min} analytically. Since the gas follows the universal track until $t_{\text{diss}}(J_{21}) < \min(t_{\text{rec}}, t_{\text{cool}})$,

we can solve the equation:

$$t_{\text{diss}} = \min(t_{\text{rec}}, t_{\text{cool}}) \quad (22)$$

to obtain the temperature T_{min} at which the H_2 is dissociated and the gas stops cooling (this argument only holds for $J_{21}/n < 1.5 \times 10^{-2}$. For $J_{21}/n > 1.5 \times 10^{-2}$ then $t_{\text{diss}} < t_{\text{cool}}$ always holds. The gas can nonetheless cool by a small amount, which must be calculated by solving the energy equation). We plot the result as points in Figure 6. The simple estimate $t_{\text{diss}} = t_{\text{cool}}$ shows remarkably good agreement with the results of the full chemistry code.

4.2.2. The cooled gas fraction in halos

The significance of the previous result is as follows. In order for the gas to cool down to a temperature T_{min} , it must have $(\frac{J_{21}}{n}) < (\frac{J_{21}}{n})_{\text{crit}}$; in particular, in the presence of a given dissociating flux J_{21} , the gas must have $n > n_{\text{crit}}$. In halos with $T_{\text{vir}} < 10^4 \text{K}$, H_2 is the only available coolant; if initially $n < n_{\text{crit}}$ the gas will never cool to T_{min} . For this reason, H_2 formation and cooling is thought to be inhibited in $T < 10^4 \text{K}$ halos due to the effects of an external UV dissociating background (Haiman, Rees & Loeb 1997, Ciardi et al. 2000, Haiman, Abel & Rees 2000, Machacek et al. 2001). However, the effects of an external UV background are much less severe for $T > 10^4 \text{K}$ halos, primarily because atomic cooling contracts the gas to sufficiently high densities that the H_2 formation and cooling timescales are shorter than the photodissociation time. Initially, when the gas density is low, H_2 formation will be suppressed, and the gas will cool by atomic cooling, contracting until $n > n_{\text{crit}}$ and H_2 cooling takes over. From Figure 6, we see that in order to cool the gas down to $\sim 500 \text{K}$, we require $n > n_{\text{crit}} \sim 10^3 J_{21} \text{cm}^{-3}$.

From equations (1) and (3) we see that almost all of the baryons in the disk will satisfy this criterion (as the gas cools it will be compressed further, increasing the gas fraction which satisfies $n > n_{\text{crit}}$). By contrast, in $T_{\text{vir}} < 10^4 \text{K}$ halos, where there is no means of initially compressing the gas, only a small fraction of the gas exists at $n > n_{\text{crit}}$. We can quantify this statement by assuming that the gas in $T_{\text{vir}} < 10^4 \text{K}$ halos is initially isothermal at the virial temperature of the halo. The density profile of the gas is then given by demanding hydrostatic equilibrium in an NFW halo (Makino et al. 1998). We adopt this profile to compute the fraction of baryonic mass of a halo above a given number density $M_b(> n)$. Halos which collapse at similar redshift are roughly self-similar, and have a fixed fraction of their mass above a given density, independent of their mass.

In Figure 7, we compute the fraction of gas which can cool down to a temperature T for halos at $z = 15$, as a function of the external UV radiation field J_{21} . For comparison, the radiation field corresponding to n_γ ionizing photons per baryon in the universe is $J_{21} \approx \frac{h_P c}{4\pi} n_\gamma n_b (1+z)^3 \times 10^{21} \approx 10 n_\gamma \left(\frac{1+z}{16}\right)^3$ (where n_b is the comoving baryon number density, and h_P is the Planck constant). Only an extremely small fraction of the gas can cool to low temperatures $T < 500 \text{K}$ required for a reasonably small Jeans mass, $M_J = 10^4 (T/500 \text{K})^{3/2} (n/10^4 \text{cm}^{-3})^{-1/2} \text{M}_\odot$.

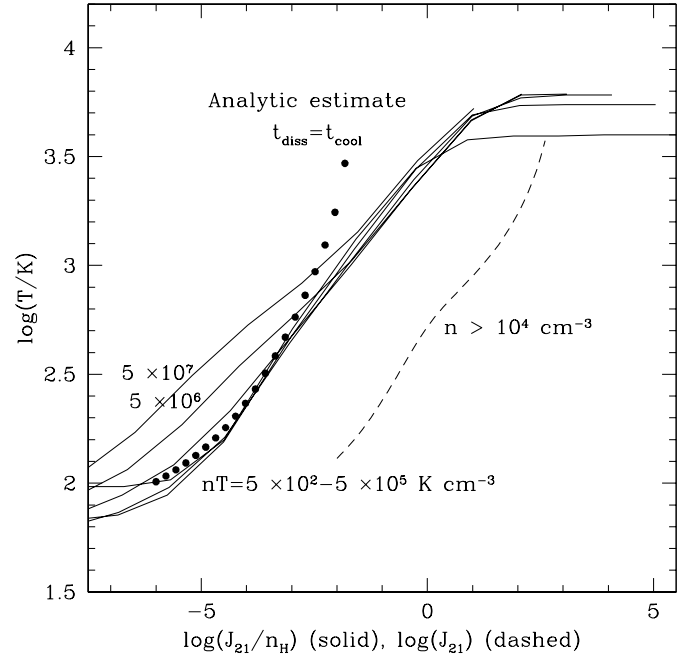


FIG. 6.— The minimum temperature T_{min} a gas parcel can cool down to, as a function of J_{21}/n , for $nT = 5 \times 10^2, 10^3, 10^4, 10^5, 10^6, 10^7 \text{K cm}^{-3}$ (solid curves). These results were obtained by integrating the rate equations for an isobarically cooling parcel of gas. The cooling depends only on a single variable $J_{21}/n \propto t_{\text{cool}}/t_{\text{diss}}$; this can be seen from the fact that almost all the curves lie on top of one another. This scaling behaviour is only broken when the gas approaches high densities $n > 10^4 \text{cm}^{-3}$ (i.e., the $nT = 5 \times 10^6, 5 \times 10^7 \text{K cm}^{-3}$ curves) at which point the cooling time becomes independent of density and $t_{\text{cool}}/t_{\text{diss}} \propto J_{21}$. In this case, the minimum temperature the gas can cool down is not given by J_{21}/n but by J_{21} alone (dashed line). The points represent the analytic estimate of T_{min} as a function of J/n by setting $t_{\text{diss}} = t_{\text{cool}}$; in the range $J/n < 1.5 \times 10^{-2}$ where this estimate is valid, the agreement with the full calculation is remarkably good.

A similar quantity has been computed by Machacek et al. (2001) in numerical simulations of halo formation and gas cooling. In their Figure 3, they plot the fraction of gas f_{gas} that has cooled to $T < 0.5 T_{\text{vir}}$ and $\rho > \rho_{\text{threshold}}$ as a function of T_{vir} and find a strong correlation between f_{gas} and T_{vir} . The reason for this is that the cooling function of H_2 depends strongly on T . Since the cooling function $\Lambda_{\text{H}_2} \propto T^4$ is much greater at higher T , n_{crit} is correspondingly lower for high T_{vir} halos and thus f_{gas} is higher. We find reasonable agreement (to within a factor of two in the cold mass fraction), if we plot our results in this fashion. Here we choose to compute the fraction which cools to a fixed temperature T , since ultimately it is the final temperature which determines the Jeans mass. By our criterion, there is no correlation of f_{gas} with T_{vir} . By comparison, virtually all of the disk gas in halos with $T_{\text{vir}} > 10^4 \text{K}$ halos can cool to low temperatures $T < 500 \text{K}$, due to the high densities in the disk. Overall, while levels of flux comparable to that required for the universe to be fully reionized will strongly suppress cooling in $T_{\text{vir}} < 10^4 \text{K}$ halos, they have negligible impact on H_2 formation and cooling in $T_{\text{vir}} > 10^4 \text{K}$ halos.

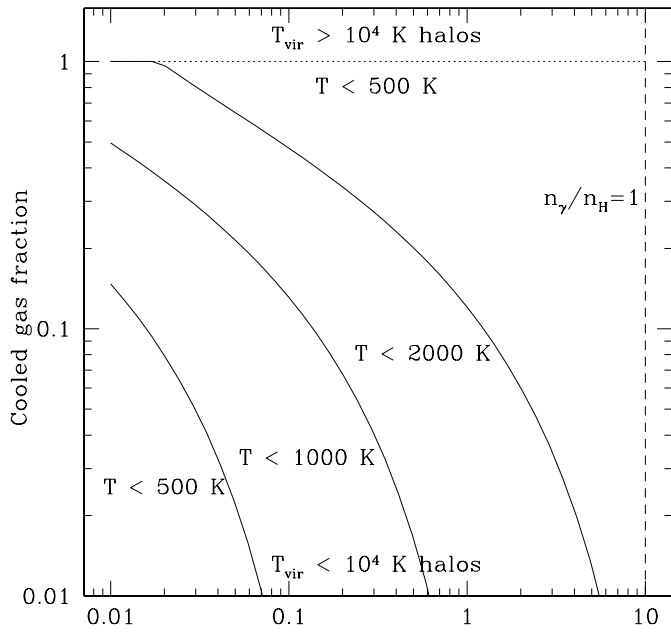


FIG. 7.— The fraction of gas in a halo that can cool below a given temperature as a function of the external UV radiation field, for halos at $z=15$. The radiation field corresponding to 1 ionizing photon per baryon in the universe is marked. In halos with $T_{\text{vir}} < 10^4 \text{ K}$ (solid lines), only a small fraction of the gas is at sufficiently high density to be unaffected by external radiation fields. By contrast, in halos where atomic cooling operates, the gas contracts to such high densities that virtually all of the disk gas can form H_2 and cool to low temperatures.

4.2.3. Self-shielding

We now consider the role of self-shielding. We have previously seen that gas in disks can form H_2 and cool for all reasonable values of the external UV radiation field even if we neglect self-shielding. We therefore confine ourselves to a few general remarks. Self-shielding is much more important in $T_{\text{vir}} > 10^4 \text{ K}$ halos than in lower mass halos: after the gas has settled in the disk, column densities are higher by a factor $\lambda^{-2} \sim 400$. If H_2 forms with the asymptotic abundance of $x_{\text{H}_2} \sim 10^{-3}$, then from equation (4), the H_2 column density is: $N_{\text{H}_2}(r) \approx 10^{20} \exp(-r/2R_d) \left(\frac{f_d}{0.5}\right) \left(\frac{T_{\text{vir}}}{5 \times 10^4 \text{ K}}\right)^{1/2} \left(\frac{\lambda}{0.05}\right)^{-2} \left(\frac{1+z}{10}\right)^{3/2} \text{ cm}^{-2}$.

There are two extremes cases to be considered. If the gas is static $v/b \ll 1$, then the LW flux is attenuated by a factor: $f_{sh} = \min \left[1, \left(\frac{N_{\text{H}_2}}{10^{14} \text{ cm}^{-2}} \right)^{-0.75} \right] \ll 1$ (Draine & Bertoldi 1996; this fitting formula is accurate to within a factor of 2 for $N_{\text{H}_2} < 5 \times 10^{20} \text{ cm}^{-2}$, at which point the LW flux is attenuated by 5 orders of magnitude). In this regime, self-shielding is extremely strong and the gas is impervious to external UV radiation. However, if there are significant velocity gradients with $v/b \gg 1$, then the gas remains optically thin to LW radiation until the damping wings of the LW lines overlap, at $N_{\text{H}_2} \approx 10^{22} \text{ cm}^{-2}$ (Draine & Bertoldi 1996, Glover & Brand 2000; in particular, see Fig. 2 and 3 of Glover & Brand 2000, where the fraction of radiation in the LW bands absorbed is computed as a function of H_2 column density. For $N_{\text{H}_2} \sim 10^{20} \text{ cm}^{-2}$, only $\sim 10\%$ of the radiation is absorbed). The magnitude of self-shielding therefore depends on the velocity field of the

gas, which probably lies closer to the $v/b \gg 1$ regime, particularly as the disk cools by H_2 cooling to temperatures $T_{\text{gas}} \ll T_{\text{vir}}$, and thus $b \ll V_{\text{circ}}$. We have seen that gas in the disk is unaffected by photodissociating UV radiation even if self-shielding is unimportant. On the other hand, the H_2 optical depth affects the efficiency of H_2 dissociation by internal sources; if the optical depth is high, then a large fraction of the energy emitted in the LW bands by stars goes towards dissociating H_2 . We now turn to H_2 photodissociation by internal UV sources.

4.3. Photodissociation by internal UV radiation

H_2 photodissociation by internal sources is likely to be the dominant source of feedback. Following Glover & Brand (2000), we can estimate the dissociation efficiency as follows. A single 100 M_\odot metal free star produces $\dot{N}_{\text{dis}} \sim 10^{49} \text{ photons s}^{-1}$ in the 11.15-13.6 eV range. Let us assume that a fraction $f_{\text{abs}} \sim 0.1$ of these photons are absorbed in the disk (as is appropriate if $N_{\text{H}_2} \sim 10^{20} \text{ cm}^{-2}$; see Figures 2 & 3 in Glover & Brand 2000) and $f_{\text{dis}} \sim 0.2$ of excitations lead to dissociations. Then over its main sequence lifetime $t_{\text{ms}} \sim 3 \times 10^6 \text{ yr}$, the star will dissociate $M_{\text{gas}} \approx f_{\text{dis}} f_{\text{abs}} m_{\text{H}_2} \dot{N}_{\text{dis}} t_{\text{ms}} / x_{\text{H}_2} \sim 10^7 \text{ M}_\odot$ of gas of all its H_2 , assuming $x_{\text{H}_2} \sim 10^{-3}$ (see also Omukai & Nishi (1999)). This could imply a star formation efficiency as low as $f_{\text{star}} \sim 10^{-5}$.

The efficiency with which cooling and star formation can still proceed depends on the amount of clumping and fragmentation that can take place before internal sources of radiation turn on. Dense clumps have short free-free times and may be able to collapse before all the H_2 in them is dissociated. While the H_2 in the center of a cooling clump may initially be shielded from dissociating radiation (since $N_{\text{H}_2} \gg 10^{14} \text{ cm}^{-2}$ for most clumps), ultimately if $t_{\text{diss}} \equiv M_{\text{H}_2} / \dot{M}_{\text{H}_2} < t_{\text{dyn}}$, where M_{H_2} is the mass of H_2 in the clump and \dot{M}_{H_2} is the H_2 dissociation rate, then the clump cannot collapse.

For a uniform density clump, the requirement that $t_{\text{dyn}} < t_{\text{diss}}$ translates into the requirement that the clump lie at a distance $D > 10 \left(\frac{\dot{N}_{\text{dis}}}{10^{49} \text{ s}^{-1}} \right)^{1/2} \left(\frac{n_g}{10^4 \text{ cm}^{-3}} \right)^{-7/12} \left(\frac{M_{\text{clump}}}{10^4 \text{ M}_\odot} \right)^{-1/6} \left(\frac{f_{\text{abs}}}{10^{-2}} \right)^{-1/2} \text{ pc}$ from the nearest dissociating source. By comparison, the virial radius is $r_{\text{vir}} \approx 2 \left(\frac{T_{\text{vir}}}{5 \times 10^4 \text{ K}} \right)^{1/2} \left(\frac{1+z}{10} \right)^{-3/2} \text{ kpc}$, and the disk scale length is $R_d \approx \frac{\lambda}{\sqrt{2}} r_{\text{vir}} \approx 70 \text{ pc}$. Even if H_2 is completely dissociated in the disk, it may still be possible for dense clumps to form in the halo (where the radiation field from stars is weaker), either fragmenting and forming stars in the halo itself or falling into the disk and accreting gas there.

There is a hard limit to the temperature a parcel of gas exposed to dissociating radiation can cool to. This is because at high densities $n > 10^4 \text{ cm}^{-3}$, collisional excitation and de-excitation dominate, the gas falls into LTE, and the cooling time becomes independent of density. We can find this minimum temperature by setting $t_{\text{cool}}(x_{\text{H}_2}, T) = t_{\text{diss}}(J_{21})$ for the universal H_2 fraction $x_{\text{H}_2} \sim 10^{-3}$. The result is shown in Figure 6 (dashed curve). If the dissociating flux exceeds a critical value of $J > J_{\text{crit}} \approx 10^3$, then cooling below $\sim 4000 \text{ K}$ is impossible, independent of the density of the gas. Such flux levels

are easily attainable from internal stellar radiation fields: a 100M_\odot metal free star would generate a radiation field $J_{21} \approx 10^3 \left(\frac{\dot{N}_{\text{dis}}}{10^{49} \text{s}^{-1}} \right) \left(\frac{D}{20 \text{pc}} \right)^{-2}$ in the LW bands. Since $D \sim 20 \text{pc}$ is of order the size of typical cooling clumps, it implies that once a single star forms within a clump, subsequent cooling and fragmentation within the clump will be suppressed.

If internal photodissociation is a very efficient source of feedback, then star formation initiated by H_2 cooling cannot take place in the disk, and is likely to proceed only in the halo (where the sources of radiation are spread farther apart). If the disk has sufficiently low spin to be Toomre unstable at $\sim 10^4 \text{K}$, then unstable clumps could form in the disk, cooling isothermally by atomic cooling. As long as they can cool to extremely high densities ($n > 10^{12} \text{cm}^{-3}$), then stellar-mass size clumps could still form. Omukai (2001) has suggested that the gas cools initially by $\text{Ly}\alpha$ and two photon emission for $n < 10^7 \text{cm}^{-3}$, and then by free-bound emission from H^- until $n \sim 10^{16} \text{cm}^{-2}$, when the gas becomes optically thick to continuum radiation. This cooling route does not permit the formation of H_2 by three-body reactions at high densities when cooling from high initial temperatures. Unless sufficient H_2 can form initially to cool the gas down to $T < 2000 \text{K}$, collisional dissociation completely overwhelms the three-body H_2 formation rate (see rates by Galli, Palla & Salpeter 1982). We have found the equilibrium values of H_2 for $T > 5000 \text{K}$ to be negligibly small, even for extremely high densities $n \gg 10^8 \text{cm}^{-3}$. In principle, clumps cooling via atomic cooling could cool to sufficiently high densities so as to reach sub-solar fragmentation masses (Omukai 2001). This leads to a somewhat counterintuitive possibility: within photodissociation regions where $J_{21} > 10^3$ and H_2 formation and cooling is suppressed, the fragmentation masses could be *smaller* than in regions where H_2 formation and cooling can take efficiently.

A possible obstacle to contraction to such high densities is radiation pressure from $\text{Ly}\alpha$ photon scattering; we examine this issue in the next subsection. If the majority of disks are Toomre stable and photodissociation by internal UV sources is very efficient, then efficient star formation may have to await not just $T > 10^4 \text{K}$ halos, but halos capable of self-enriching themselves in metals, with sufficiently deep potential wells that metals ejected by supernovae rain back down on the disk in a galactic fountain, rather than being lost to the IGM. From local observations, the critical circular velocity appears to be $v \sim 130 \text{km s}^{-1}$ (Martin 1999). For metal-free stars radiative mass loss is likely to be inefficient (Kudritzki 2000), and except for stars which collapse directly to black holes and do not eject metals, \sim half the stellar mass is converted to metals (Heger & Woosley 2001). Thus, the fraction of gas processed into stars roughly corresponds to the metallicity enrichment, $f_{\text{star}} \sim Z$. Studies of gas cooling (Hellsten & Lin 1997, Bromm et al. 2001b) suggest that $Z \sim 10^{-3} \text{Z}_\odot \sim 10^{-5}$ is the critical metallicity at which metal line cooling allows the gas to cool down to $T < 100 \text{K}$, implying that a prior star formation efficiency of $f_{\text{star}} > 10^{-5}$ is required with H_2 cooling before metal line cooling can take over. This seems compatible (given the many uncertainties) with our estimate of $f_{\text{star}} \sim 10^{-5}$.

4.4. $\text{Ly}\alpha$ photon trapping and radiation pressure

Collapse and fragmentation can be halted if the opacity of the contracting gas rises sufficiently that the energy density of trapped radiation becomes high and radiation pressure support becomes important. The condition for this to occur is:

$$Lt_{\text{trap}} > E_{\text{bind}} \approx \frac{GM^2}{R} \quad (23)$$

where L is the luminosity of the radiation source, t_{trap} is the timescale on which photons are trapped within the collapsing cloud, and E_{bind} is the binding energy of the cloud. If the only source of radiation is cooling radiation and the system is in free fall collapse, then $L \approx E_{\text{bind}}/t_{\text{dyn}}$ and condition (23) translates into the condition $t_{\text{trap}} > t_{\text{dyn}}$. Rees & Ostriker (1977) have emphasized that if the only radiation source is cooling, then even if all radiation is trapped, radiation pressure cannot halt an overall collapse, since the resulting energy density is only half that required to support the cloud ($P_{\text{gas}} = 2/3U_{\text{gas}}$, but $P_{\text{rad}} = 1/3U_{\text{rad}}$; in addition, in our case \sim half of the energy is radiated in the two photon continuum, rather than in the $\text{Ly}\alpha$ line, and can escape more easily). Nonetheless, they note that radiation pressure could become sufficiently important so as to boost the Jeans mass and halt fragmentation. We now investigate this possibility, and also consider the case when an internal radiation source provides additional photons to provide pressure support.

When the system is isothermally contracting by atomic cooling at $\sim 8000 \text{K}$ and the gas is largely neutral, the dominant opacity source is $\text{Ly}\alpha$ scattering. The optical depth at line center to escaping $\text{Ly}\alpha$ photons across a contracting clump of mass $M_J \approx 3 \times 10^5 \left(\frac{T}{8000 \text{K}} \right)^{3/2} \left(\frac{n_g}{10^4 \text{cm}^{-3}} \right)^{-1/2} \text{M}_\odot$ is $\tau = 1.2 \times 10^{10} \left(\frac{n_g}{10^4 \text{cm}^{-3}} \right) \left(\frac{r}{7 \text{pc}} \right)$, which is enormous. However, due to the finite line width the photons diffuse in both space and frequency, escaping from the cloud when they have scattered sufficiently far from line center. This problem has been investigated by a number of authors (Adams 1975, Neufeld 1990), who find:

$$t_{\text{trap}} = 15 t_{\text{cross}} \quad 10^3 \leq \tau \leq 10^6$$

$$t_{\text{trap}} = 15 t_{\text{cross}} \left(\frac{\tau}{10^6} \right)^{1/3} T_4^{1/6} \quad \tau \geq 10^6 \quad (24)$$

where $t_{\text{cross}} = R/c$ is the light crossing time. In addition, Bonilha et al. (1979) find from Monte Carlo calculations that dust and velocity gradients reduce the trapping time by a factor $f_{\text{dust}} = \frac{1}{(1+0.9\delta)^{0.97}}$ and $f_v = \frac{1}{1+0.027\eta^{1.5}}$ respectively, where $\delta = \frac{t_{\text{trap}}}{t_{\text{cross}}} \tau_{\text{dust}}$ and $\eta \approx 1.5 \left(\frac{\Delta V}{b} \right)$, where ΔV is the velocity gradient across the cloud and b is the Doppler parameter. Since we only consider gas of almost zero metallicity ($Z < 10^{-3} \text{Z}_\odot$) we ignore the effects of dust; in addition, since we have $\Delta V \sim b$ and thus $f_v \sim 1$, velocity gradients are unimportant. From equation (24) we find that at $n \sim 10^4 \text{cm}^{-3}$ then $t_{\text{trap}} \approx 350 t_{\text{cross}} \approx 8 \times 10^{-3} t_{\text{dyn}}$, and radiation pressure is unimportant. If the clump does not fragment and $nr^3 = \text{const}$, then $t_{\text{trap}}/t_{\text{dyn}} \propto n^{8/18} \propto M^{-8/9}$ and thus at $n \sim 5 \times 10^8 \text{cm}^{-3}$, when $M_J \sim 10^3 \text{M}_\odot$, radiation pressure could potentially become comparable to the thermal gas pressure. In particular, radiation pres-

sure could significantly impede the contraction of a massive clump of gas.

In reality, the gas is likely to fragment as it cools. If we only consider the photon diffusion time across a Jeans length, then for isothermal cooling $M_J \propto nR_J^3 \propto n^{-1/2}$, i.e. $R_J \propto n^{-1/2}$. This yields $t_{\text{trap}}/t_{\text{dyn}} \propto n^{1/6} \propto M^{-1/3}$. In this case, the Jeans mass can fall far below a solar mass before radiation pressure ever becomes important.

We now consider the case where an internal ionizing source, such as stars or QSOs provide additional Ly α photons from their HII regions, and consider whether collapse and fragmentation in the (largely neutral) gas beyond the surrounding regions can be halted by radiation pressure. Consider a cooling clump of mass M_J at $T = 10^4$ K. In order for $P_{\text{rad}} = \frac{1}{3}U_{\text{rad}} \approx \frac{1}{3}\frac{L_{\text{Ly}\alpha}t_{\text{trap}}}{V} > P_{\text{therm}} = nk_{\text{b}}T$, we require:

$$\dot{N}_{\text{Ly}\alpha} \approx \dot{N}_{\text{ion}} > 4 \times 10^{50} \left(\frac{M_J}{10^6 M_{\odot}} \right)^{1/3} \text{ photons s}^{-1} \quad (25)$$

where we assume that each ionizing photon results in the production of a Ly α photon. By comparison, for metal free stars with $M_* > 100 M_{\odot}$, we have $\dot{N}_{\text{ion}} \sim 10^{50} \left(\frac{M_*}{100 M_{\odot}} \right)$ photons s $^{-1}$ (Tumlinson & Shull 2000, Bromm et al. 2001c); therefore, only $\sim 10^{-3}$ of the mass of a $10^6 M_{\odot}$ clump need fragment into such stars for radiation pressure to become important. However, this is still unlikely to completely prevent smaller subclumps from collapsing. The critical star formation efficiency required to maintain $P_{\text{rad}} = P_{\text{gas}}$ as a function of the Jeans mass is

$$f_{\text{star}} \equiv \frac{\rho_*}{\rho_{\text{g}}} \approx 10^{-3} \left(\frac{M_J}{10^6 M_{\odot}} \right)^{-2/3}. \quad (26)$$

Thus, when $M_J \sim 300 M_{\odot}$, $f_{\text{star}} \sim 100\%$ of the gas must fragment into stars to halt collapse. We conclude that Ly α photon pressure from stars can halt the overall contraction of a cooling cloud, but it does not maintain the Jeans mass above a certain mass scale. Smaller subclumps have shorter trapping times and require unattainably high internal Ly α photon production rates to halt collapse. However, Ly α pressure is likely to act as a feedback mechanism regulating the efficiency with which such clumps collapse, since it prevents the ambient medium from cooling and condensing to high densities.

In particular, radiation pressure from stars or AGN can significantly retard or halt the free fall collapse of the gas; if cooling gas becomes radiation pressure supported, then entropy fluctuations will be smoothed out and further fragmentation could be very inefficient. This could well imply star formation efficiencies of order that given by equation (26). Ly α photon pressure could regulate the accretion of gas onto a dense clump, as well as increase the scale height of the disk. It is therefore likely to be an important source of feedback until supernova explosions become dominant. A full quantitative investigation of the effects of Ly α photon trapping in the early universe is beyond the scope of this paper (previous authors have studied the effects of radiation pressure in related contexts; see, e.g., Cox 1985; Bithell 1990; Haehnelt 1995).

5. CONCLUSIONS

In this paper, we have examined the cooling of gas in the first halos at high redshift with $T_{\text{vir}} > 10^4$ K, which are able to cool via atomic line cooling. Previous generations of halos with $T_{\text{vir}} < 10^4$ K, in which the only available coolant is H₂ molecules, are expected to have their cooling strongly suppressed by feedback processes (Haiman, Abel & Rees 2000; Omukai & Nishi 1999). Thus, the gas in these larger halos is likely to still be of nearly primordial composition. Our main findings can be summarized as follows:

1. The gas should cool isothermally initially and settle toward a rotationally supported disk at the center of the dark matter halo. Unless the halo has unusually low angular momentum or a large fraction ($f_{\text{d}} > 0.5$) of the gas cools to form the disk (by contrast, present day dwarfs typically only have $f_{\text{d}} \sim 0.3$), the majority of such disks will be gravitationally stable by the Toomre criterion. An additional coolant is therefore required to lower the gas sound speed and promote gravitational instability. We identify this coolant as H₂.
2. In gas which has been collisionally ionized and heated to a temperature of $T > 10^4$ K, H₂ molecules form with a universal fraction $x_{\text{H}_2} \sim 10^{-3}$, independent of initial density or temperature for a wide range of initial conditions. This universal fraction is not an equilibrium value. Rather, it can be understood as the result of a 'freeze-out'. The H₂ formation and destruction timescale become long compared to all other timescales at a temperature $T_{\text{freeze}} \sim 3700$ K; $x_{\text{H}_2} \sim 10^{-3}$ thus reflects the equilibrium value of H₂ at T_{freeze} , the temperature at which the H₂ abundance stops evolving. Independence of density can be understood from the fact that all collisional timescales scale as $\propto 1/n$, and thus the ratio of timescales is independent of density; in particular, the gas follows a universal track in the (x_e, T) plane. Independence of the initial temperature can be understood from the fact that the gas recombines isothermally at ~ 9000 K, losing memory of the initial conditions.
3. We have examined the feedback from UV radiation fields and conclude that H₂ photodissociation from an external UV background, comparable to that required to reionize the universe, is unlikely to be important. This is because atomic cooling contracts the gas to such high initial densities that the H₂ formation and cooling timescales are shorter than the UV photodissociation timescales. This is in contrast to $T < 10^4$ K halos where only a small fraction of H₂ at the center of the halo is at sufficiently high density to promote cooling within a photodissociation time; the fraction of gas in such halos which cools is much lower. We argue that radiation pressure due to Ly α photon trapping could conceivably limit the efficiency of star formation. This is because only a small fraction of the gas needs to be converted into stars for a collapsing clump to become radiation pressure supported. Another possible source of pres-

sure support, which we have not examined, arises from turbulent velocity fields (Padoan 1995).

While the fact that H_2 can form out of metal-free gas cooling from $T > 10^4 \text{K}$ and cool the gas to $\sim 10^2 \text{ K}$ is a robust result, we stress that our picture of how this enables gas to settle into cold, gravitationally unstable disks at the center of halos is considerably more uncertain. At stake is not only a large variation in the efficiency of star formation in low mass halos and thus the redshift of reionization (see Figures 1 and 2), but also the mass scale at which clumps form, which bears upon the stellar IMF and perhaps upon the question of supermassive black hole formation. In particular, the degree of fragmentation of the gas is highly uncertain. These important questions can only be addressed with some degree of confidence by high-resolution numer-

ical simulations which are able to track the detailed gas hydrodynamics, chemistry and cooling, paralleling the pioneering work already done for $T_{\text{vir}} < 10^4 \text{K}$ halos (Abel et al. 2000, Bromm et al. 2001a). The main hope of this paper is to stimulate further work along these lines.

We thank D. Neufeld and T. Abel for useful comments; Volker Bromm, Jordi Miralda-Escudé, Andrey Kravtsov, and Martin Rees for stimulating conversations; and Joop Schaye for correcting a factor of 2 error. SPO was supported by NSF grant AST-0096023. ZH was supported by NASA through the Hubble Fellowship grant HF-01119.01-99A, awarded by the Space Telescope Science Institute, which is operated by the Association of Universities for Research in Astronomy, Inc., for NASA under contract NAS 5-26555.

REFERENCES

Abel, T., Anninos, P., Norman, M. L., & Zhang, Y. 1997, *NewA*, 2, 181
 Abel, T., Bryan, G. L., & Norman, M. L. 2000, *ApJ*, 540, 39
 Abel, T., & Haiman, Z., 2000, in "H₂ in Space", proceedings of the conference held at Paris, France, September 1999, eds. F. Combes and G. Pineau des Forets, p. 237
 Allison, A. C. & Dalgarno, A. 1970, *Atomic Data*, 1, 289
 Bahcall, N.A., Ostriker, J. P., Perlmutter, S., & Steinhardt, P. J. 1999, *Science*, 284, 1481
 Adams, T. F. 1975, *ApJ*, 201, 350
 Barkana, R., & Loeb, A., 2001, *Physics Reports*, in press, astro-ph/0010468
 Barnes, J., & Efstathiou, G. 1987, *ApJ*, 319, 575
 Binney, J., & Tremaine, S. 1987, *Galactic Dynamics*, Princeton Univ. Press, Princeton, pp. 362-365
 Black, J. H. 1978, *ApJ*, 222, 125
 Blumenthal, G. R., Faber, S. M., Flores, R., & Primack, J. R. 1986, *ApJ*, 301, 27
 Bithell, M., 1990, *MNRAS*, 244, 738
 Bonilha, J. R. M., Ferch, R., Salpeter, E. E., Slater, G., & Noedlinger, P. D. 1979, *AJ*, 233, 649
 Bromm, V., Coppi, P.S., & Larson, R.B., 2001a, *ApJ*, submitted, astro-ph/0102503
 Bromm, V., Ferrara, A., Coppi, P. S., & Larson, R. B. 2001b, *MNRAS*, submitted, astro-ph/0104271
 Bromm, V., Kudritzki, R.P., & Loeb, A. 2001c, *ApJ*, 552, 464
 Cen, R. 1992, *ApJ*, 78, 341
 Ciardi, B., Ferrara, A., Governato, F., & Jenkins, A., 2000, *MNRAS*, 314, 611
 Cox, D.P., 1985, *ApJ*, 288, 465
 Corbelli, E., & Salpeter, E. E. 1995, *ApJ*, 450, 32
 Dalgarno, A., & Lepp, S. 1987, in *Astrochemistry: Proceedings of IAU Symposium No. 120*, ed. M. S. Vary & S. P. Tarafdar, Reidel Publishing Co., Dordrecht, p. 109
 Dalgarno, A. & Stephens, T. L. 1970, *ApJ*, 160, L107
 de Jong, T. 1972, *A&A*, 20, 263
 Dove, J. E., & Mandy, M. E. 1986, *ApJ*, 311, 93
 Draine, B. T., & Bertoldi, F., 1996, *ApJ*, 468, 269
 Efstathiou, G., 2000, *MNRAS*, 317, 697
 Ferrara, A. 1998, *ApJ*, 499, L17
 Flores, R., Primack, J. R., Blumenthal, G. R., & Faber, S. M. 1993, 412, 443
 Galli, D., & Palla, F. 1998, *A&A*, 335, 403
 Glover, S.C.O., & Brand, P.W.J.L. 2001, *MNRAS*, 321, 385
 Goldreich, P., & Lynden-Bell, D. 1965, *MNRAS*, 130, 97
 Haiman, Z., Abel, T., & Rees, M. J. 2000, *ApJ*, 534, 11
 Haiman, Z., & Loeb, A. 1998, *ApJ*, 503, 505
 Haiman, Z., Rees, M. J., & Loeb, A. 1996, *ApJ*, 467, 522
 Haiman, Z., Rees, M. J., & Loeb, A. 1997, *ApJ*, 476, 458
 Haiman, Z., Spaans, M., & Quataert, E., 2000, *ApJ*, 537, L5
 Haardt, F., Madau, P. 1996, *ApJ*, 461, 20
 Haehnelt, M. G. 1995, *MNRAS*, 273, 249
 Heger, A., & Woosley, S.E., 2001, *ApJ*, submitted, astro-ph/0107037
 Hellsten, U., & Lin, D. N. C., *ApJ*, submitted, astro-ph/9708086
 Hirasawa, T. 1969, *Prog. Theor. Phys.*, v. 42, no. 3, p. 523
 Hutchings, R. M., Santoro, F., Thomas, P. A., & Couchman, H. M. P. 2001, *MNRAS*, submitted, astro-ph/0102117
 Jimenez, R., Heavens, A. F., Hawkins, M. R. S., & Padoan, P. 1997, *MNRAS*, 292, L5
 Kang, H., & Shapiro, P. R. 1992, *ApJ*, 386, 432
 Karpas, Z., Anicich, V., and Huntress, W. T. 1979, *J. Chem. Phys.*, 70, 2877
 Kashlinsky, A., & Rees, M.J., 1983, *MNRAS*, 205, 955
 Kennicutt, R. C., Jr. 1989, *ApJ*, 344, 685
 Kudritzki, R.P., 2000, in *The First Stars*, Weiss, A., Abel, T., Hill, V. (eds), Springer, Berlin, p. 127
 Lepp, S., & Shull, J. M. 1983, *ApJ*, 270, 578
 Machacek, M. E., Bryan, G. L., Abel, T. 2001, *ApJ*, 548, 509
 MacLow, M.-M., Ferrara, A., 1999, *ApJ*, 513, 142
 Madau, P., & Rees, M. J. 2001, *ApJL*, in press, astro-ph/0101223
 Makino, N., Sasaki, S., & Suto, Y. 1998, *ApJ*, 497, 555
 Martin, C.L., 1999, *ApJ*, 513, 156
 Mo, H.J., Mao, S. & White, S.D.M. 1998, *MNRAS*, 295, 319
 Nakashima, K., Takayi, H., Nakamura, H. 1987, *J. Chem. Phys.*, 86, 726
 Navarro, J. F., Frenk, C. S., & White, S. D. M. 1997, *ApJ*, 490, 493
 Navarro, J., & Steinmetz, M., 2000, *ApJ*, 538, 477
 Navarro, J., & White, S.D.M., 1993, *MNRAS*, 265, 271
 Neufeld, D. A. 1991, *ApJ*, 370, 85
 Oh, S.P., 2001, *ApJ*, 553, 499
 Omukai, K., 2001, *ApJ*, 546, 635
 Omukai, K., & Nishi, R. 1999, *ApJ*, 518, 64
 Osterbrock, D. E., 1989, *Astrophysics of Gaseous Nebulae and Active Galactic Nuclei*, University Science Books, Sausalito, CA
 Padoan, P., 1995, *MNRAS*, 277, 377
 Rawlings, J. M. C., Drew, J. E., Barlow, M. J. 1993, *MNRAS*, 265, 968
 Rees, M. J., & Ostriker, J. P. 1977, *ApJ*, 179, 541
 Ricotti, M., Gnedin, N.Y., & Shull, J.M., 2000, *ApJ*, submitted, astro-ph/0012335
 Ricotti, M., Gnedin, N.Y., & Shull, J.M., 2001a, *ApJ*, submitted, astro-ph/0110431
 Ricotti, M., Gnedin, N.Y., & Shull, J.M., 2001b, *ApJ*, submitted, astro-ph/0110432
 Shapiro, P. R., & Kang, H. 1987, *ApJ*, 318, 32
 Spitzer, L., Jr. 1942, *ApJ*, 95, 329
 Spitzer, L., Jr., 1978, *Physical Processes in the Interstellar Medium*, John Wiley & Sons, p. 143
 Susa, H., Uehara, H., Nishi, R., Yamada, M., 1998, *PThPh*, 100, 63
 Thacker, R.J., & Couchman, H.M.P., *ApJ*, in press, astro-ph/0106060
 Tumlinson, J., & Shull, M.J. 2000, *ApJ*, 528, L65
 van den Bosch, F. C., Burkert, A., & Swaters, R. A. 2001, *MNRAS*, submitted, astro-ph/0105082
 Venkatesan, A., Giroux, M.L., Shull, J.M., 2001, *ApJ*, in press, astro-ph/0108168
 Warren, M. S., Quinn, P. J., Salmon, J. K., & Zurek, W. H. 1992, 339, 405
 Weil, M.L., Eke, V.R., & Efstathiou, G., 1998, *MNRAS*, 300, 773
 White, S. D. M., & Rees, M. J. 1978, *MNRAS*, 183, 341

APPENDIX: REACTION RATES AND CROSS SECTIONS

Reaction	Rate Coefficient ($\text{cm}^3 \text{ sec}^{-1}$)	Reference
----------	---	-----------

(1)	$H + e^- \rightarrow H^+ + 2e^-$	$5.85 \times 10^{-11} T^{\frac{1}{2}} \exp(-157809.1/T) (1 + T_5^{\frac{1}{2}})^{-1}$	[1]
(2)	$He + e^- \rightarrow He^+ + 2e^-$	$2.38 \times 10^{-11} T^{\frac{1}{2}} \exp(-285335.4/T) (1 + T_5^{\frac{1}{2}})^{-1}$	[2]
(3)	$He^+ + e^- \rightarrow He^{++} + 2e^-$	$5.68 \times 10^{-12} T^{\frac{1}{2}} \exp(-631515.0/T) (1 + T_5^{\frac{1}{2}})^{-1}$	[1]
(4)	$H^+ + e^- \rightarrow H + h\nu$	$8.40 \times 10^{-11} T^{-\frac{1}{2}} T_3^{-0.2} (1 + T_6^{0.7})^{-1}$	[1]
(5)	$He^+ + e^- \rightarrow He + h\nu$	see expression in reference	[1]
(6)	$He^{++} + e^- \rightarrow He^+ + h\nu$	$3.36 \times 10^{-10} T^{-\frac{1}{2}} T_3^{-0.2} (1 + T_6^{0.7})^{-1}$	[1]
(7)	$H + H^+ \rightarrow H_2^+ + h\nu$	see expression in reference	[3]
(8)	$H_2^+ + H \rightarrow H_2 + H^+$	6.40×10^{-10}	[4]
(9*)	$H + e^- \rightarrow H^- + h\nu$	$1.4 \times 10^{-18} T^{0.928} \exp(-T/16200)$	[5]
(10)	$H + H^- \rightarrow H_2 + e^-$	1.30×10^{-9}	[6]
(11)	$H_2^+ + e^- \rightarrow 2H$	$1.68 \times 10^{-8} (T/300)^{-0.29}$	[7]
(12)	$H_2^+ + H^- \rightarrow H_2 + H$	$5.00 \times 10^{-6} T^{-\frac{1}{2}}$	[8]
(13*)	$H^- + H^+ \rightarrow 2H$	$5.7 \times 10^{-6} T^{-\frac{1}{2}} + 6.3 \times 10^{-8} - 9.2 \times 10^{-11} T^{\frac{1}{2}} + 4.4 \times 10^{-13} T$	[5]
(14)	$H_2 + e^- \rightarrow H + H^-$	$2.70 \times 10^{-8} T^{-\frac{3}{2}} \exp(-43000/T)$	[9]
(15*)	$H_2 + H \rightarrow 3H$	$1.067 \times 10^{-10} \left(\frac{T}{\text{eV}}\right)^{2.012} \exp[-4.463(\frac{T}{\text{eV}})^{-1}] / (1 + 0.2472(\frac{T}{\text{eV}})^{3.512})$	[10]
(16)	$H_2 + H_2 \rightarrow H_2 + 2H$	see expression in reference	[11]
(17*)	$H_2 + H^+ \rightarrow H_2^+ + H$	$3 \times 10^{-10} \exp(-21050/T) \ (T_4 < 1); 1.5 \times 10^{-10} \exp(-14000/T) \ (T_4 \geq 1)$	[5]
(18)	$H_2 + e^- \rightarrow 2H$	$4.38 \times 10^{-10} \exp(-102000/T) T^{0.35}$	[12]
(19)	$H^- + e^- \rightarrow H + 2e^-$	$4.00 \times 10^{-12} T \exp(-8750/T)$	[12]
(20)	$H^- + H \rightarrow 2H + e^-$	$5.30 \times 10^{-20} T^{2.17} \exp(-8750/T)$	[12]
(21)	$H^- + H^+ \rightarrow H_2^+ + e^-$	see expression in reference	[12]

Cross-section (cm²)

(22)	$H + h\nu \rightarrow H^+ + e^-$	$6.3 \times 10^{-18} \left(\frac{13.6\text{eV}}{h\nu}\right)^4 \exp(4 - 4(\tan^{-1}\epsilon/\epsilon)) / [1 - \exp(-2\pi/\epsilon)]; \epsilon \equiv \sqrt{\frac{h\nu}{13.6} - 1}$	[13]
(23*)	$He + h\nu \rightarrow He^+ + e^-$	$0.694 \times 10^{-18} \left[\left(\frac{h\nu}{\text{eV}}\right)^{1.82} + \left(\frac{h\nu}{\text{eV}}\right)^{3.23}\right]^{-1}$	[14]
(24)	$He^+ + h\nu \rightarrow He^{++} + e^-$	$1.575 \times 10^{-18} \left(\frac{54.4\text{eV}}{h\nu}\right)^4 \exp(4 - 4(\tan^{-1}\epsilon/\epsilon)) / [1 - \exp(-2\pi/\epsilon)]; \epsilon \equiv \sqrt{\frac{h\nu}{54.4} - 1}$	[13]
(25*)	$H^- + h\nu \rightarrow H + e^-$	$7.928 \times 10^5 (\nu - \nu_T)^{\frac{3}{2}} \nu^{-3}$ for $h\nu \geq h\nu_T = 0.755 \text{ eV}$	[15]
(26*)	$H_2^+ + h\nu \rightarrow H + H^+$	see expression in reference	[12]
(27)	$H_2 + h\nu \rightarrow H_2^+ + e^-$	see expression in reference	[12]
(28)	$H_2 + h\nu \rightarrow 2H$	$\sigma(\nu) = 3 \times 10^{-18}$ for $11.26 \text{ eV} < h\nu < 13.6 \text{ eV}$	[16]

1. Cen (1992); 2. Black (1978); 3. Rawlings et al. (1993); 4. Karpas et al. (1979); 5. Galli and Palla (1998); 6. de Jong (1972); 7. Nakashima et al. (1987); 8. Dalgarno & Lepp (1987); 9. Hirasawa (1969); 10. Dove & Mandy (1986); 11. Lepp & Shull (1983); 12. Shapiro & Kang (1987); 13. Osterbrock (1974); 14. Haardt & Madau 1996; 15. Abel et al. (1997); 16. Allison & Dalgarno (1970) and Dalgarno & Stephens (1970).

The table above lists the chemical reactions included in our chemistry network. For reference, we have marked (with a “*”) the reactions whose adopted rates are different from the compilation in Haiman, Rees & Loeb (1996).